

Article

Mapping the Orthosteric Binding Site of the Human 5-HT Receptor Using Photo-crosslinking Antagonists

Thomas Jack, Michele Leuenberger, Marc-David Ruepp, Sanjeev Kumar V Vernekar, Andrew J Thompson, Sophie Braga-Lagache, Manfred Heller, and Martin Lochner

ACS Chem. Neurosci., Just Accepted Manuscript • DOI: 10.1021/acscchemneuro.8b00327 • Publication Date (Web): 27 Aug 2018

Downloaded from <http://pubs.acs.org> on August 28, 2018

Just Accepted

"Just Accepted" manuscripts have been peer-reviewed and accepted for publication. They are posted online prior to technical editing, formatting for publication and author proofing. The American Chemical Society provides "Just Accepted" as a service to the research community to expedite the dissemination of scientific material as soon as possible after acceptance. "Just Accepted" manuscripts appear in full in PDF format accompanied by an HTML abstract. "Just Accepted" manuscripts have been fully peer reviewed, but should not be considered the official version of record. They are citable by the Digital Object Identifier (DOI®). "Just Accepted" is an optional service offered to authors. Therefore, the "Just Accepted" Web site may not include all articles that will be published in the journal. After a manuscript is technically edited and formatted, it will be removed from the "Just Accepted" Web site and published as an ASAP article. Note that technical editing may introduce minor changes to the manuscript text and/or graphics which could affect content, and all legal disclaimers and ethical guidelines that apply to the journal pertain. ACS cannot be held responsible for errors or consequences arising from the use of information contained in these "Just Accepted" manuscripts.



ACS Publications

is published by the American Chemical Society, 1155 Sixteenth Street N.W., Washington, DC 20036

Published by American Chemical Society. Copyright © American Chemical Society. However, no copyright claim is made to original U.S. Government works, or works produced by employees of any Commonwealth realm Crown government in the course of their duties.

Mapping the Orthosteric Binding Site of the Human 5-HT₃ Receptor Using Photo-crosslinking Antagonists

Thomas Jack,[†] Michele Leuenberger,^{†,¶} Marc-David Ruepp,^{†,&} Sanjeev Kumar V. Vernekar,^{#,⊥} Andrew J. Thompson,[‡] Sophie Braga-Lagache,[§] Manfred Heller,[§] and Martin Lochner^{*,†,¶}

[†]Department of Chemistry and Biochemistry, University of Bern, Freiestrasse 3, 3012 Bern, Switzerland.

[#]Department of Chemistry, University of Warwick, Coventry CV4 7AL, UK.

[‡]Department of Pharmacology, University of Cambridge, Tennis Court Road, Cambridge CB2 1PD, UK.

[§]Department of BioMedical Research, Mass Spectrometry and Proteomics Laboratory, University of Bern, Inselspital, 3010 Bern, Switzerland.

[¶]Institute of Biochemistry and Molecular Medicine, University of Bern, Bühlstrasse 28, 3012 Bern, Switzerland.

Abstract

The serotonin-gated 5-HT₃ receptor is a ligand-gated ion channel. Its location at the synapse in the central and peripheral nervous system have rendered it a prime pharmacological target, e.g. for antiemetic drugs that bind with high affinity to the neurotransmitter binding site and prevent the opening of the channel. Advances in structural biology techniques has led to a surge of disclosed three-dimensional receptor structures, however, solving ligand-bound high-resolution 5-HT₃ receptor structures has not been achieved to date. Ligand binding poses in the orthosteric binding site have been largely predicted from mutagenesis and docking studies. We report the synthesis of a series of photo-crosslinking compounds

whose structures are based on the clinically used antiemetic drug granisetron (Kytril®). These displaced [³H]granisetron from the orthosteric binding site with low nanomolar affinities and showed specific photo-crosslinking with the human 5-HT₃ receptor. Detailed analysis by protein-MS/MS identified a residue (Met-228) near the tip of binding loop C as the covalent modification site.

Key Words: 5-HT₃ receptor; antagonist; granisetron; photo-crosslinking probe; orthosteric binding site; mass spectrometry; docking

Introduction

The serotonergic system is involved in the control and regulation of many physiological processes such as sleep, appetite, vasoconstriction, body temperature, gastrointestinal motility and mood. With respect to the latter, an imbalanced function of the serotonergic system has been strongly associated with depression and mood disorders. Several drugs on the market (e.g. selective serotonin reuptake inhibitors, SSRIs), aim to improve this imbalance, albeit with varying success. Serotonin (5-hydroxytryptamine, 5-HT) is a neurotransmitter that exerts its effect by activating at least fourteen different receptors. The large majority of these are metabotropic (5-HT_{1,2,4-7}), while only the 5-HT₃ receptor is ionotropic and responsible for the fast depolarization of neurons.¹⁻³ As such, the 5-HT₃ receptor shares more structural similarities with other members of the Cys-loop ligand-gated ion channel family that also includes nicotinic acetylcholine (nACh), γ -amino butyric acid (GABA_{A/C}) and glycine receptors. These ion channels consist of five subunits that are pseudo-symmetrically assembled around a central ion conducting pore. Each of the five protomers features three structurally distinct domains (Figure 1a): the extracellular domain (ECD), the transmembrane domain (TMD) and the intracellular domain (ICD). The serotonin binding sites (i.e. orthosteric sites) are located in the ECD at the interface of two adjacent protomers, formed by the convergence of three peptide loops from one protomer (the

principal face, loops A-C) and three loops from the neighboring protomer (the complementary face, loops D-F, Figure 1c).⁴

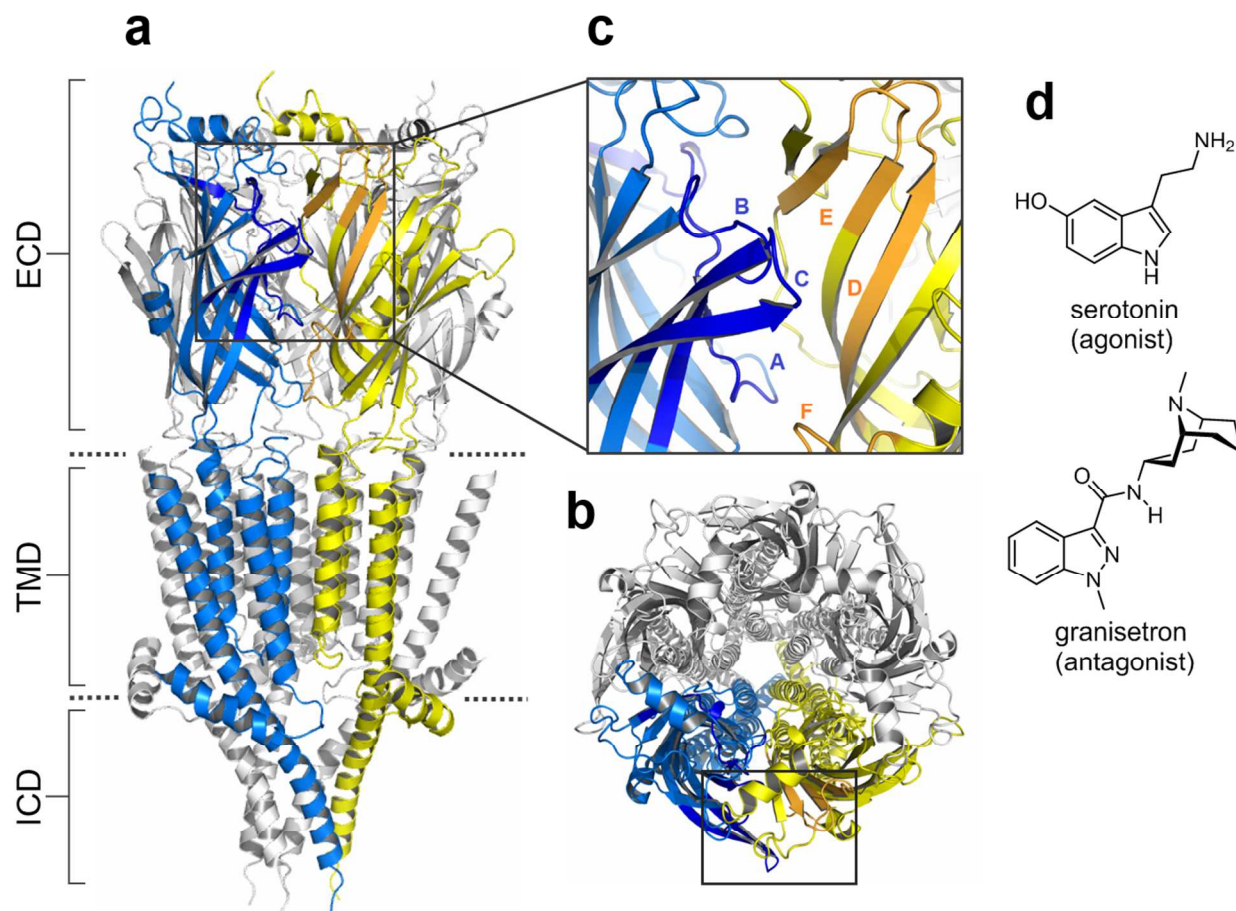


Figure 1. (a) View parallel to the plasma membrane of the mouse 5-HT_{3A} receptor (PDB ID: 4PIR) with the extracellular (ECD), transmembrane (TMD) and intracellular (ICD) domains indicated. The stabilizing nanobodies have been omitted for clarity. The approximate location of the lipid bilayer is shown by horizontal dotted lines. Two adjacent protomers forming one orthosteric binding site (black box) are highlighted. (b) Extracellular view perpendicular to the plasma membrane of the receptor with one orthosteric binding site (black box) indicated. (c) Close up view of one orthosteric binding site showing the principal face (blue, loops A-C) and complementary face (yellow, loops D-F). (d) Chemical structures of endogenous agonist serotonin and prototypical competitive antagonist granisetron (Kytril®).

A class of high-affinity antagonists (the ‘setrons’) that compete with serotonin for the orthosteric 5-HT₃ receptor binding sites has been established as anti-emetic drugs in the clinic, alleviating the symptoms of nausea and vomiting resulting from chemo-, radiotherapy and general anaesthesia.³ Pharmacological antagonism of 5-HT₃ receptors is also used to treat irritable bowel syndrome (IBS). Recent reports indicate, however, that partial 5-HT₃ receptor agonism might be a better approach to treat certain types of IBS, as a large group of patients suffer from significant side effects during the current antagonist treatment.⁵ Other disorders where 5-HT₃ receptors might be involved include depression, drug abuse, schizophrenia, fibromyalgia, pruritus, bulimia nervosa and pain.⁶⁻⁸

Detailed structural information about the 5-HT₃ receptor binding sites would be very beneficial for the development of novel compounds to improve current therapies and establish new therapies in other disease areas. A wealth of mutagenesis studies in the past three decades have probed putative binding site residues that often have been deduced from a combination of homology modelling and docking.⁹⁻¹¹ These and other studies have identified residues that are important for ligand binding and/or channel gating, although extracting detailed non-covalent interactions between functional groups of the ligand and receptor residues is very challenging. Four years ago the first crystal structure of a mammalian 5-HT₃ receptor was presented (Figure 1).¹² The truncated form of the homomeric mouse 5-HT_{3A} receptor was stabilized with nanobodies and its structure solved to a resolution of 3.5 Å (PDB ID: 4PIR). In this apo structure, the recognition loops of the nanobodies reach into the orthosteric binding site. More recently, the cryo-EM structure of the full length mouse apo-5-HT_{3A} receptor at 4.3 Å resolution was published (PDB ID: 6BE1).¹³ In a different approach, pentameric acetylcholine binding protein (AChBP), that is homologous to the ECD, was engineered to bind agonists and antagonists with affinities comparable to the 5-HT₃ receptor (termed 5HTBP). One such construct was co-crystallized with competitive antagonist granisetron (PDB ID: 2YME)¹⁴ and with picomolar-affinity antagonist palonosetron (PDB ID: 5LXB),¹⁵ and the complexes were solved to high resolution (2.4 Å and 2.3 Å, respectively). These models have

revealed very detailed non-covalent interactions, such as hydrogen bonds, hydrophobic, π - π and cation- π interactions, between the ligands and binding site residues. Nevertheless, one has to exercise caution when using these binding site models to predict binding orientations of structurally similar ligands at the receptor.¹⁶

Using photo-crosslinking probes is a well-established technique to capture weak non-covalent interactions between a small molecule and its target protein. In the Cys-loop receptor family, orthosteric and allosteric binding sites on nACh and GABA receptors have been investigated by utilizing photo-crosslinking probes, derived from general anesthetics, insecticides and other modulators, in conjunction with protein sequence analysis after labelling (e.g. MS).¹⁷⁻²⁴ Moreover, covalent labelling can also be utilized to map the binding site(s) of a ligand or to identify the cellular target(s) if unknown. Photo-crosslinking moieties such as diazirines, benzophenones and phenylazides that are appended to a tolerant position of the bioactive molecule are most commonly employed.^{25,26} The photo-crosslinking methodology is applicable to native, wild type proteins and if the design of the probe is chosen appropriately (e.g. by using a modifiable linker or additional bioorthogonal functional groups) the target protein can be functionalized further with new properties by way of post-photoaffinity modification (P-PALM).^{27,28} However, only a few photo-crosslinking studies have been conducted with 5-HT₃ receptors. For instance, Blanton and co-workers have employed the lipophilic, well-known photolabel [¹²⁵I]TID (3-trifluoromethyl-3-(*m*-[¹²⁵I]iodophenyl)diazirine) to covalently modify receptor residues at the lipid-protein interface.²⁹ Earlier studies by Lummis and Baker have also shown that intrinsically photo-reactive antipsychotic phenothiazines label the 5-HT₃ receptor orthosteric binding site, however, a detailed post-labelling sequence analysis was not performed.³⁰ Therefore, detailed structural information from photo-labelling could be beneficial for understanding the binding of ligands at these receptors.

We have previously developed fluorescent³¹⁻³³ and PET³⁴ 5-HT₃ receptor ligands derived from the high-affinity, competitive antagonist granisetron (Kytril®, Figure 1d) and used these probes to study these receptors in cells and live animals. Here we extend these studies of biophysical probes by

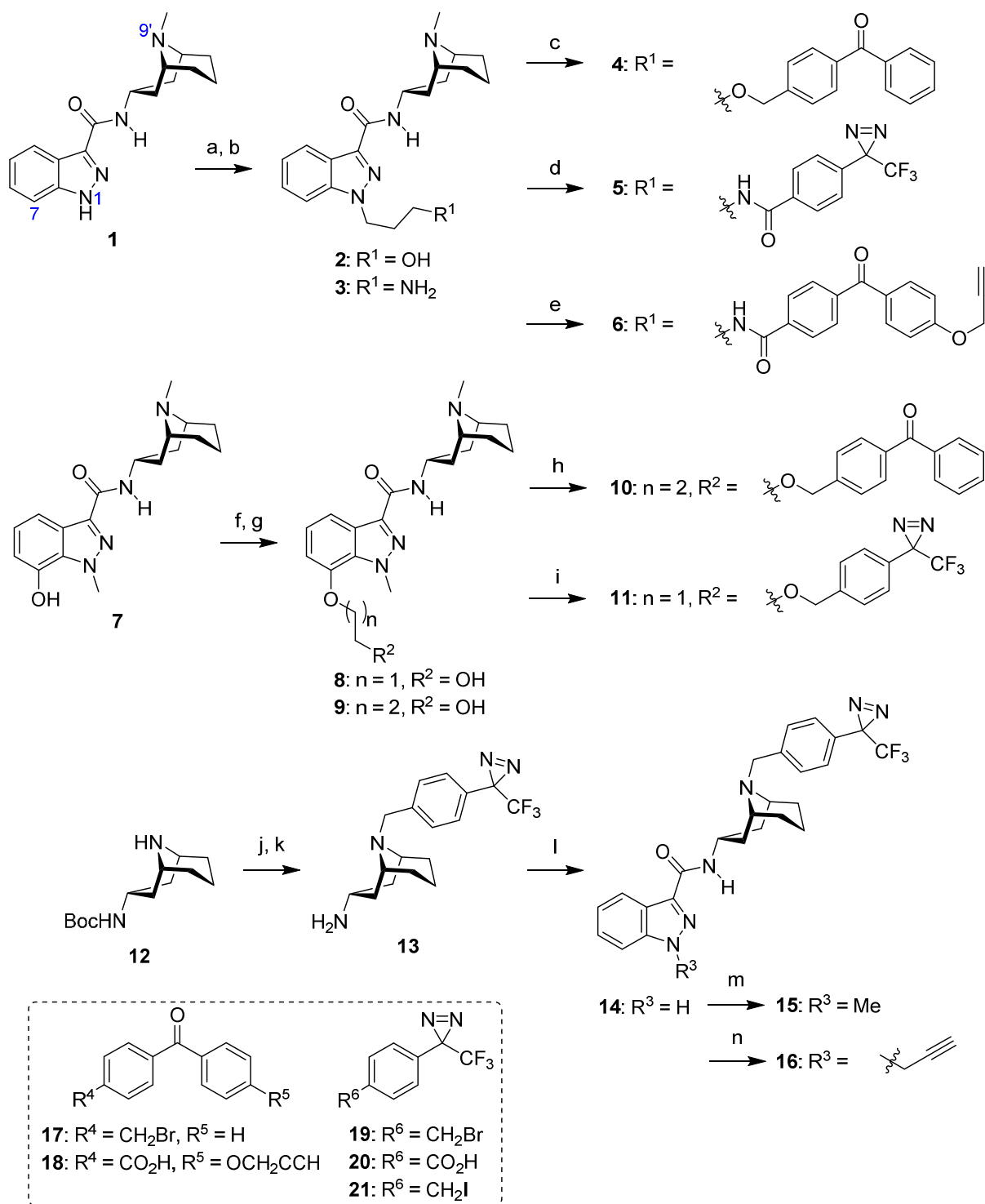
synthesizing a series of photo-crosslinking probes that were created by appending various photo-reactive moieties to three different positions of the granisetron core. Furthermore, we use these probes to specifically photo-label residues in the orthosteric binding site of the 5-HT₃ receptor.

Results and Discussion

Design and Synthesis of 5-HT₃ Receptor Photo-crosslinking Probes

Following our previous SAR study of granisetron³⁵ and design of fluorescent granisetron probes^{31,32} we chose to link the photo-labelling moieties to the indazole *N*-1, C-7 or granatane *N*-9' position of the antagonist core (Scheme 1). Briefly, either 1*H*-indazole amide **1**³⁵ or 7-hydroxyindazole amide **7**^{31,35} were alkylated with protected linkers, followed by deprotection and subsequent alkylation with benzophenone bromide **17**³⁶ or diazirine benzyl bromide **19**,³⁷ or amidation with diazirine benzoic acid **20**.^{38,39} For accessing the *N*-9' modified probes **15** and **16**, Boc-protected granatane amine **12**⁴⁰ was alkylated first with diazirine benzyl iodide **21**,^{41,42} deprotected, coupled to 1*H*-indazole-3-carboxylic acid and finally *N*-1 alkylated.

We have also synthesized two granisetron probes **6** and **16** that, in addition to the photo-labelling moieties, contain an alkyne handle to aid post-photoaffinity identification of modified receptors by means of Cu(I)-catalysed alkyne-azide cycloaddition (CuAAC) reactions. Granisetron probe **6** was obtained through amidation of precursor **3**³⁵ with benzophenone acid **18**^{43,44} and **16** was synthesized by *N*-1 propargylation of indazole amide **14**.



Scheme 1. Synthesis of granisetron-based photo-crosslinking probes. Reagents and conditions: (a) KO^tBu , THF/DMF 5:1, $0^\circ C$; either $Br(CH_2)_3OTBS$ or $Br(CH_2)_3NHBoc$, rt, 68% ($R^1 = OTBS$), 78% ($R^1 = NHBoc$). (b) For $R^1 = OTBS$: TBAF, THF, rt, 86% **2**. For $R^1 = NHBoc$: 1.2M HCl in MeOH, rt, 98% **3**.

(c) **2**, NaH, THF/DMF 5:1, 0°C; **17**, rt, 27%. (d) **3**, **20**, Et₃N, HATU, DMF/DCM 3:2, rt, 24%. (e) **18**, SOCl₂, MeCN, 80°C; **3**, DCM, 0°C to rt, 11%. (f) KO^tBu, THF/DMF 5:1, 0°C; either Br(CH₂)₂OTBS or Br(CH₂)₃OTBS, rt, 78% (*n* = 1), 34% (*n* = 2). (g) TBAF, THF, rt, 51% **8** (*n* = 1), 85% **9** (*n* = 2). (h) **9**, NaH, THF/DMF 5:1, 0°C; **17**, rt, 20%. (i) **8**, NaH, THF/DMF 5:1, 0°C; **19**, rt, 35%. (j) K₂CO₃, **21**, EtOH, 55°C, 82%. (k) TFA, DCM, rt, quant. (l) 1*H*-indazole-3-carboxylic acid, DCC, HOBT, DCM/DMF 3:2, rt; **13**, 66%. (m) **14**, KO^tBu, THF/DMF 4:1, 0°C; MeI, rt, 88%. (n) **14**, Cs₂CO₃, DMF, rt; 3-bromoprop-1-yne, 93%. See structure **1** for the numbering of the granisetron core.

Pharmacological Characterization of 5-HT₃ Receptor Photo-crosslinking Probes

The binding affinities of the granisetron photo-crosslinking probes **4-6**, **10**, **11**, **15** and **16** for the human homopentameric 5-HT₃A receptor were assessed by competition with [³H]granisetron. The *K_i* values are summarized in Table 1.

All probes except **15** and **16** exhibited a sub-nanomolar to low nanomolar affinity at the orthosteric binding site of the 5-HT₃A receptor. This is in line with our previous findings where appendage of bulky fluorescent dyes to the indazole *N*-1 and C-7 positions resulted in high-affinity orthosteric ligands (for the numbering of the granisetron core see structure **1**, Scheme 1).^{31,32,35} Although **15** and **16** compete with [³H]granisetron for the same binding site, their affinities are three orders of magnitude lower than the parent ligand. Previously we synthesized *N*-9'-benzyl granisetron³⁵ that similarly had a lower affinity (*pK_i* = 6.72 ± 0.24, *K_i* = 191 nM, *n* = 6)¹⁶ than the parent ligand and thus it seems that further substitution at the *para*-position of the phenyl ring is less favorable.

Table 1. Binding Affinities of Granisetron Photo-crosslinking Probes at Human 5-HT₃A Receptor

| Compound | pK_i^a | K_i (nM) | n |
|-------------|--------------|-------------------|-----|
| Granisetron | - | 1.45 ^b | 3 |
| 4 | 10.21 ± 0.38 | 0.06 | 4 |
| 5 | 8.26 ± 0.04 | 5.50 | 4 |
| 6 | 7.48 ± 0.16 | 33.1 | 5 |
| 10 | 9.34 ± 0.11 | 0.46 | 4 |
| 11 | 8.22 ± 0.28 | 6.03 | 3 |
| 15 | 5.67 ± 0.14 | 2138 | 7 |
| 16 | 5.99 ± 0.22 | 1023 | 3 |

^aData are the mean of n independent experiments ± SEM and determined from competition binding with [³H]granisetron using HEK293 cell membranes stably expressing 5-HT₃AR. ^bReference ⁴⁵.

Photo-crosslinking of 5-HT₃ Receptor with Granisetron Probes

Whole cell lysate from HEK293T cells stably expressing human N-terminal FLAG-tagged 5-HT₃A receptor³² was incubated with either **6**, **16** or non-specific alkyne benzophenone **22** (Figure 2), irradiated (at 302 nm for 30 min) and subsequently treated with biotin azide **23** (Figure 2) under CuAAC conditions (CuSO₄, TBTA, TCEP). Biotinylated proteins were pulled down with streptavidin beads, eluted and analyzed by Western blot. Whereas clear biotinylated bands could be observed for **6** in the right mass region for the 5-HT₃A receptor (calc. 57.4 kDa for one protomer, exact sequence see Figure S3), photo-crosslinking with probe **16** resulted in almost no bands (Figure S1). This could be due to the significantly lower binding affinity of **16** compared to **6** (Table 1) or that differing binding orientations result in different photo-crosslinking and biotin labelling efficacies. Benzophenone **22**, that is lacking the

granisetron moiety did not give significant photo-crosslinking bands, consistent with its lack of competition with [^3H]granisetron.

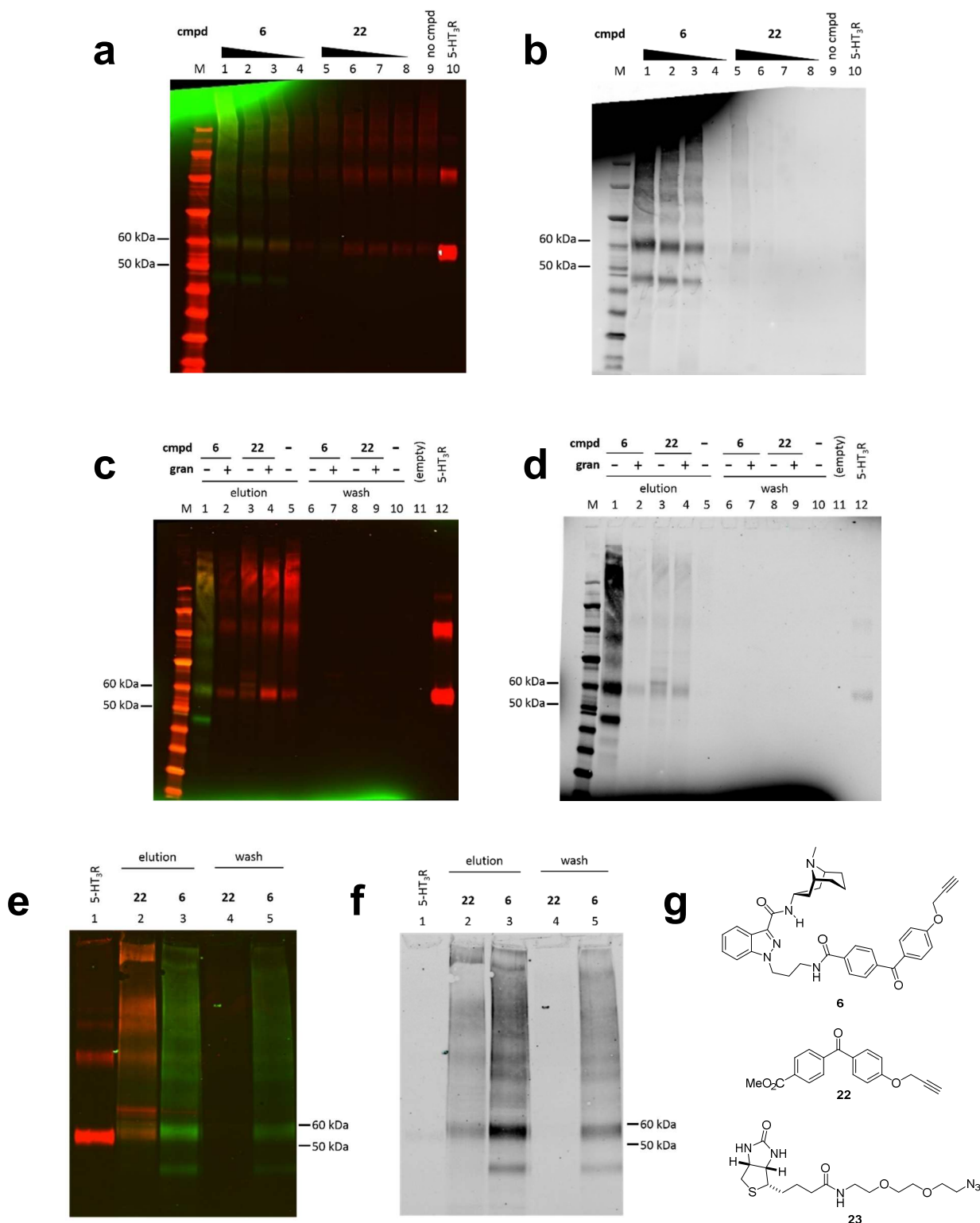


Figure 2. Photo-crosslinking of FLAG-tagged *h5*-HT₃A receptor with granisetron probe **6** and control probe **22**. Irradiation of samples was followed by CuAAC reaction with biotin azide **23** and pull down with streptavidin beads. FLAG was visualized with rabbit α -FLAG/donkey α -rabbit-IRDye 680CW (red), biotin with streptavidin-800CW (green) on Western blots. Left panels show overlay of red and green channel detection, right panels are grayscale pictures of green channel (biotin) of the same gel. 5-HT₃R: purified, non-irradiated FLAG-tagged *h5*-HT₃A receptor for reference; band between 50 and 60 kDa corresponds to one protomer (*ca.* 57 kDa), band at higher molecular weight is glycosylated protomer or dimer.³² Wash: supernatant after incubation with streptavidin beads. Elution: sample after elution from streptavidin beads. (a, b) Irradiation of purified, micelle-solubilized *h5*-HT₃A receptor in the presence of different concentrations of **6**, **22** (from left to right: 2.5 μ M, 250 nM, 25 nM, 2.5 nM) or no compound. Biotinylated protein band below 50 kDa was not identified. (c, d) Competition of granisetron (gran) with **6** significantly diminishes formation of photo-crosslinked 5-HT₃ receptor. (e, f) **6** photo-crosslinks 5-HT₃ receptor in the plasma membrane of HEK293T cells. (g) Structures of compounds used.

Affinity-purified human FLAG-tagged 5-HT₃A receptor reconstituted in C₁₂E₉ micelles³² was incubated with varying concentrations of granisetron probe **6** or benzophenone alkyne **22** (2.5 μ M – 2.5 nM), irradiated and clicked with biotin azide **23**. Clear, concentration-dependent biotinylated bands at around 60 kDa could be observed for **6** but not for non-binder **22** (Figures 2a and 2b). Whilst photo-crosslinking with 25 nM **6** still gave a distinct band for biotinylated 5-HT₃A receptor (Figure 2b, lane 3), no such band was observed at 2.5 nM **6** (Figure 2b, lane 4), consistent with this being well below its *K_i* of 33 nM (Table 1). Blocking the receptor orthosteric binding sites with granisetron prior to incubation with **6** and irradiation reduced the formation of biotinylated 5-HT₃A receptor bands on the Western blot (Figure 2d, lane 1 vs. 2). Similar to our results from whole-cell lysates, benzophenone **22** gave very little non-specific photo-crosslinking bands in the presence or absence of granisetron (Figure 2d, lanes 3 and

4). The amount of labelling by **6** in the presence of competitor granisetron was comparable to levels of labelling observed by benzophenone alkyne **22** (Figure 2d, lanes 2-4).

The photo-crosslinking of the 5-HT₃A receptor by **6** and **22** was also studied in the plasma membrane of live HEK293T cells stably expressing the FLAG-tagged construct. Cell viability was regularly checked by automated counting throughout the irradiation period (25 min at 302 nm and 0°C) and did not change (Figure S2). After affinity purification of the 5-HT₃A receptors using FLAG-beads, they were reacted with biotin azide **23** under CuAAC conditions and analyzed by Western blot (Figures 2e and 2f). With **6**, a distinct biotinylation band was detected in the mass region for one 5-HT₃A receptor protomer (Figures 2e and 2f, lane 3), while **22** gave very weak biotinylation background signals, consistent with our experiments with purified receptors in micelles (Figure 2f, lane 2).

Mass Spectrometry Analysis of Photo-crosslinked Sites

Affinity-purified FLAG-tagged human 5-HT₃A receptor³² was run on a SDS-PAGE gel, stained with Coomassie and the band at around 57 kDa was excised. Digestion of the excised band with trypsin followed by mass spectrometry analysis of the resulting peptide fragments gave a sequence coverage of 51% (Figure S3) with the hydrophobic transmembrane sequences TM1-TM4 being particularly difficult to ionize and detect. Optimization of the digestion protocols by also utilizing proteinase K, aspartase N and endoproteinase LysC allowed the identification of 78% of the whole receptor sequence and 91% of the 5-HT₃ receptor ECD (Figure S3). This includes almost full sequence coverage of the orthosteric binding loops A-F (Figure 1).

Having established suitable experimental conditions for labelling 5-HT₃ receptors, photo-crosslinking was also attempted using probes **4**, **5**, **10**, **11** and **15**. After incubation and irradiation, Coomassie-stained bands of appropriate receptor protomer mass were excised from SDS-PAGE gels and digested using the previously optimized protocols. For **4** and **10**, mass spectrometry revealed the fragment

²²⁵EFSMESSNYAEMK²³⁸ (loop C, Figures 1c and S3) had the mass shift that corresponds to the covalent modification with the probes. Further fragmentation of this peptide by MS/MS identified Met-228 as the primary site of crosslink (Figures 3 and S4). In both cases, the peak at m/z 138.13, stemming from the fragmentation of the 9-methyl-9-azabicyclo[3.3.1]nonane (granatane) moiety of **4** and **10** (Figure S5), could be clearly detected (Figures 3b and 3c, inset). Met-228 is located close to the tip of loop C of the orthosteric binding site (Figures 1c and 4), in line with our experimental evidence that both **4** and **10** compete for the same binding site as [³H]granisetron with high affinity (Table 1).

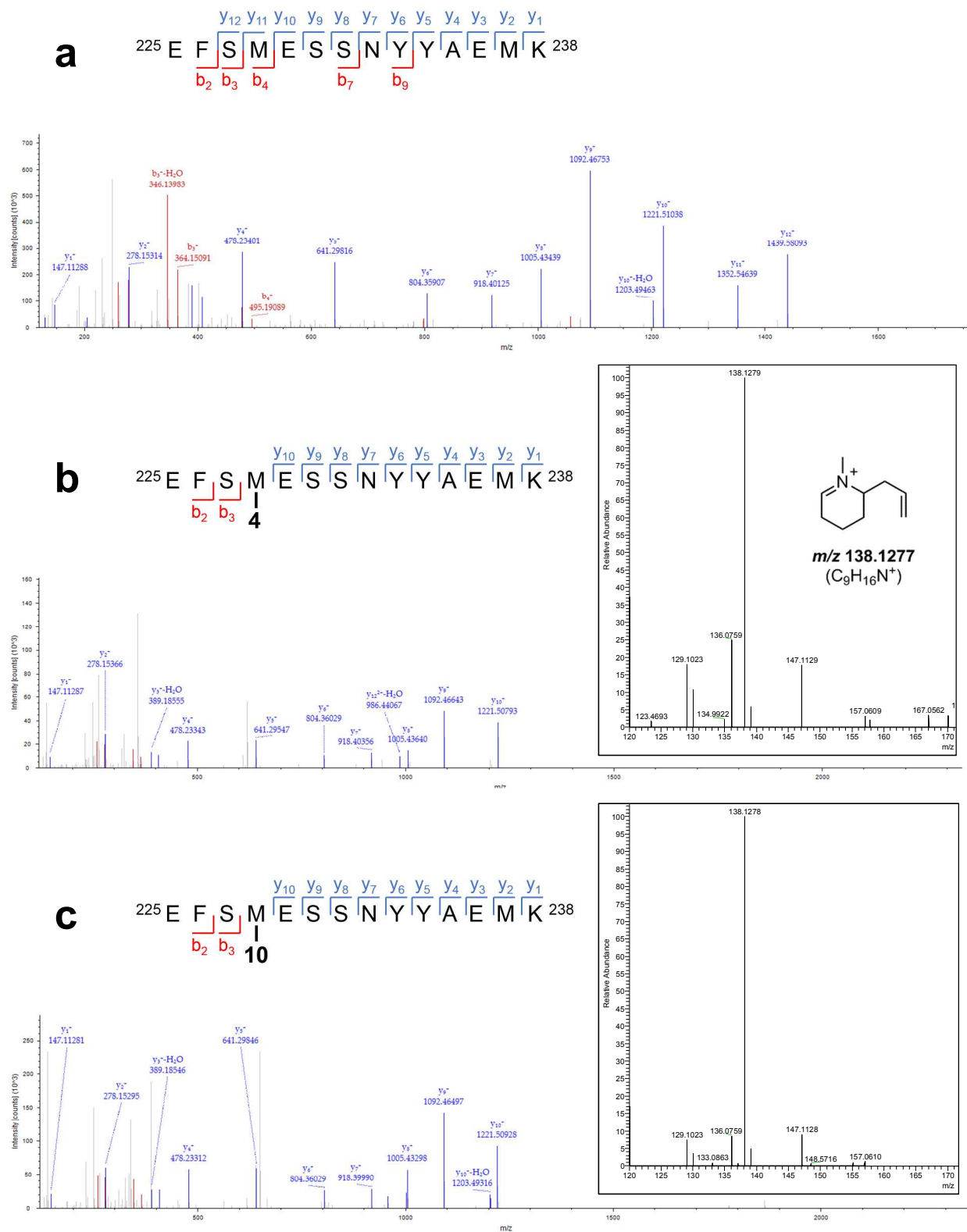


Figure 3. Identification of labelling site. Untreated (a) or probe-treated (b, c) human 5-HT₃A receptor was digested with LysC/trypsin, the resulting peptides detected by LC-MS/MS and analyzed by Sequest HT

(v1.3). Most peaks could be assigned to the y ion series of loop C (Glu-225 to Lys-238). (a) MS/MS spectrum of m/z 858.35 (unmodified peptide $^{225}\text{EFSMESSNYAEMK}^{238}$, $z = +2$). (b) MS/MS spectrum of m/z 756.00 (photo-crosslinked peptide $^{225}\text{EFSM(4)ESSNYAEMK}^{238}$, $z = +3$). Inset: Enlarged region of the spectrum showing the diagnostic $\text{C}_9\text{H}_{16}\text{N}^+$ fragment (m/z 138.13) originating from the 9-methyl-9-azabicyclo[3.3.1]nonane (granatane) moiety of the granisetron probes (Figure S5). (c) MS/MS spectrum of m/z 766.00 (photo-crosslinked peptide $^{225}\text{EFSM(10)ESSNYAEMK}^{238}$, $z = +3$). Inset: Enlarged region of spectrum. Note how in spectra (b) and (c) the y ion series is interrupted at Met-228 by the covalent modification with the probes.

Molecular Modelling

Based upon the experimental findings that **4** and **10** competitively displace [^3H]granisetron and crosslink with Met-228 of loop C we sought a computational approach to predict possible binding orientations of the two probes in the orthosteric 5-HT₃ receptor binding site. We used the high-resolution 5HTBP structure (PDB ID: 2YME) as docking template as (i) it has been mutated to mimic the human 5-HT₃ receptor binding site, (ii) the orientation of granisetron in 5HTBP is known to correctly represent the orientation found in the native 5-HT₃ receptor¹⁶ and, (iii) it was co-crystallized with granisetron which is the same recognition moiety of our probes. For the purpose of validation, granisetron was docked (FRED v2.1) into this binding site model and its predicted orientation was found to be similar to the binding pose in the crystal structure (Figure S6a). Probes **4** and **10** were also docked into the same site without restraints and resulted in the predicted binding orientations shown in Figures 4 and S7.

In light of experimental evidence, such as mutagenesis and the pharmacophore model for competitive 5-HT₃ receptor antagonists, we prefer the orientations shown in Figure 4. For both **4** and **10** the granisetron moiety is located in the middle of the orthosteric binding site between loops B, C (principal face), D and E (complementary face). The azabicyclic moiety is pointing towards the centrally

located loop B residue Trp-145 (Trp-183 in 5-HT₃ receptor, Figure S6b). This highly conserved residue can form cation- π interactions with ammonium groups^{46,47} and is known to influence the binding of several other orthosteric 5-HT₃ receptor ligands.⁴⁸ Overall, the granisetron portion of **4** and **10** broadly occupies a similar position and orientation as co-crystallized granisetron in 5HTBP (green sticks, Figure 4). The benzophenone photo-crosslinking group is near the tip of loop C with the carbonyl carbon within short distance of the side chain of Ser-187 that aligns with Met-228 in the 5-HT₃ receptor (Figure S6b). The carbonyl group of benzophenones converts into a ketyl radical upon irradiation, which can rapidly react with nearby C-H bonds forming covalent connection.²⁵ It should be noted that although the orientations in these dock-poses are compelling, to confirm the poses requires further experimental validation. Ultimately, probes **4** and **10** are photo-crosslinking conjugates of granisetron and caution may be needed when predicting binding orientations for other ligands from the poses that are shown.¹⁶

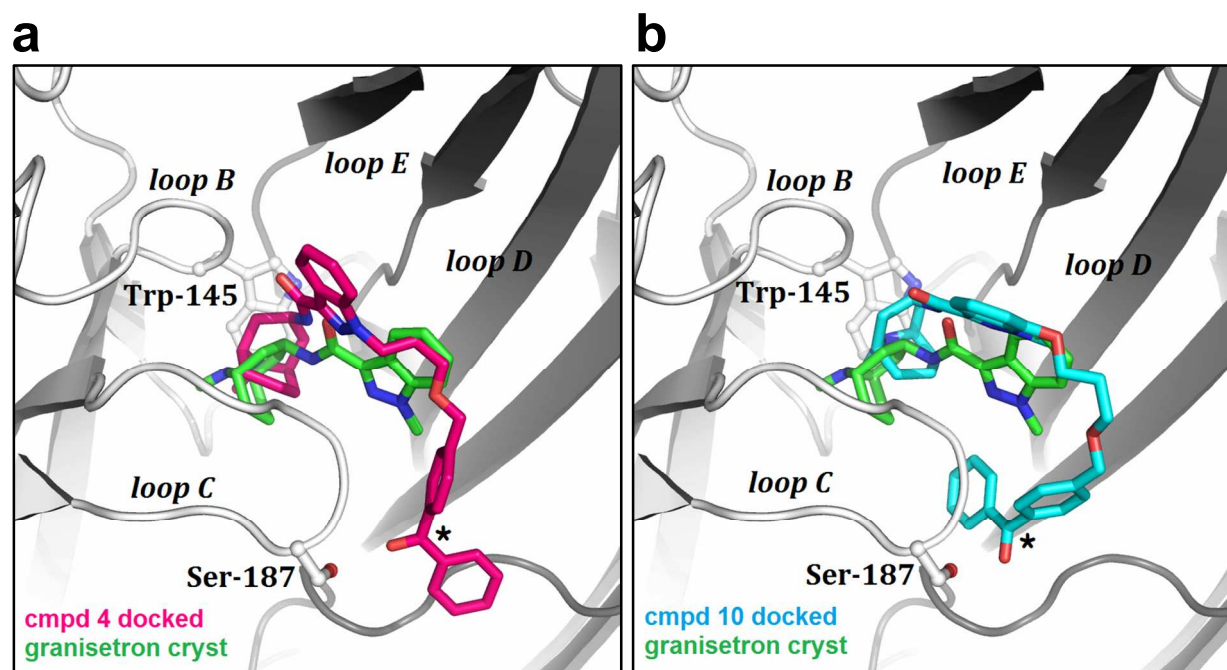


Figure 4. Proposed binding orientations of photo-crosslinking probes (a) **4** (deep pink sticks) and (b) **10** (cyan sticks) in the 5HTBP orthosteric binding site. Ligand poses shown are representative of clusters of generated docking solutions (**4**: 3/10, **10**: 2/10 of generated docking solutions) that are the most consistent with evidence from mutagenesis and the pharmacophore model for 5-HT₃ receptor ligands.^{14,16,47} The

peptide chain of the principal face (left) is shown in white and of the complementary face (right) in gray. Granisetron co-crystallized with 5HTBP (PDB ID: 2YME) is shown as reference (green sticks). Side chains of residues Trp-145 and Ser-187 discussed in the text are highlighted as ball-and-sticks. The latter residue aligns with Met-228 of the 5-HT₃ receptor (Figure S6b) that was identified as crosslinking site by MS studies (Figure 3). Black asterisk denotes the carbonyl carbon of the benzophenone photo-crosslinking moiety of **4** and **10**. For alternative predicted binding orientations of **4** and **10** see Figure S7.

Conclusions

We synthesized nanomolar affinity photo-crosslinking probes that bind to the 5-HT₃ receptor orthosteric binding site. Our results demonstrate that the granisetron scaffold is suitable for the attachment of large biophysical tags, in particular at indazole positions *N*-1 and C-7. With these probes, we were able to specifically photo-label the receptor at Met-228 which is located near the tip of loop C. Our study also provides design clues for crosslinking probes with cleavable linkers that can be used for post-photoaffinity labelling modifications with reagents such as biotin.^{27,28} Here we achieved this in both purified and native receptors providing an opportunity to introduce other biophysical reporters (e.g. small fluorescent dyes) to the tip of the highly mobile binding loop C.

Methods

Chemistry. For general synthesis methods, synthesis of photo-crosslinking moieties **18**, **20**, **21** and protected linkers see the *Supporting Information*. The synthesis of **1**, **3** and **7** was described previously.^{31,35} Protected granatane **12**⁴⁰ and photo-crosslinking moieties (**17**,³⁶ **19**³⁷) were obtained according to literature procedures, with slight modifications (*Supporting Information*).

1-(3-Hydroxypropyl)-N-((1*R*,3*r*,5*S*)-9-methyl-9-azabicyclo[3.3.1]nonan-3-yl)-1*H*-indazole-3-carboxamide (2). A suspension of indazole amide **1**³⁵ (300 mg, 1.01 mmol) in THF/DMF 5:1 (15 mL) was cooled to 0°C. KO^tBu (124 mg, 1.20 mmol) was added as suspension in dry THF (2 mL) and the mixture was stirred at 0°C for 15 min. (3-bromopropoxy)(*tert*-butyl)dimethylsilane (382 mg, 1.51 mmol) was dissolved in dry THF (2 mL) and added to the reaction mixture. Cooling was removed and the mixture stirred at RT overnight. Solvents were removed *in vacuo*, the residue taken up in H₂O (10 mL) and the aqueous mixture extracted with EtOAc (3 x 20 mL). Drying the organic layers over Na₂SO₄ and evaporation of the solvent under reduced pressure gave crude, TBS-protected indazole (322 mg, 68%) as colorless crystals. ¹H-NMR (300 MHz, CDCl₃) δ 8.39 (d, *J* = 8.1, 1H), 7.50 – 7.32 (m, 2H), 6.78 (d, *J* = 7.6, 1H), 4.66 – 4.37 (m, 3H), 3.77 – 3.48 (m, 2H), 3.10 (d, *J* = 10.1, 2H), 2.64 – 2.42 (m, 5H), 2.23 – 2.04 (m, 2H), 1.99 (br, 3H), 1.55 – 1.50 (m, 1H), 1.44 – 1.33 (m, 2H), 1.06 (d, *J* = 9.1, 2H), 0.93 (s, 6H), 0.05 (s, 9H). MS (ESI) *m/z* 471.31, [M+H]⁺.

TBS-protected indazole from above (300 mg, 0.64 mmol) and TBAF (335 mg, 1.28 mmol) were dissolved in THF (1.5 mL) and stirred overnight at RT. H₂O (8 mL) was added and the mixture extracted with DCM (3 x 20 mL). The combined organic layers were washed with H₂O (10 mL), dried over Na₂SO₄ and evaporated. After purification with flash chromatography (silica gel, gradient DCM 100% to DCM/MeOH/Et₃N 96:3:1), title compound **2** was obtained as clear oil (196 mg, 86%). ¹H-NMR (300 MHz, CDCl₃) δ 8.38 (d, *J* = 8.2, 1H), 7.51 – 7.38 (m, 2H), 7.30 – 7.23 (m, 1H), 6.92 (s, 1H), 4.67 – 4.58 (m, 1H), 4.56 (t, *J* = 6.7, 2H), 3.63 (t, *J* = 5.8, 2H), 3.22 (d, *J* = 12.0, 2H), 2.61 (s, 3H), 2.60 – 2.50 (m, 2H), 2.25 – 2.14 (m, 2H), 2.12 – 1.96 (m, 3H), 1.71 – 1.54 (m, 3H), 1.30 – 1.08 (m, 2H). HRMS *m/z* calcd for C₂₀H₂₉N₄O₂ [M+H]⁺ 357.2285, found 357.2289.

1-(3-((4-Benzoylbenzyl)oxy)propyl)-N-((1*R*,3*r*,5*S*)-9-methyl-9-azabicyclo[3.3.1]nonan-3-yl)-1*H*-indazole-3-carboxamide (4). Alcohol **2** (33.4 mg, 93 μmol) was dissolved in anhydrous THF/DMF 5:1 (6 mL) and cooled to 0°C. NaH (8.3 mg, 208 μmol, 60% in oil) was added and stirring at 0°C was continued for 5 min. Benzophenone bromide **17** (28.4 mg, 103 μmol) was added, the cooling removed

and the suspension stirred at RT overnight. As reaction control by TLC still showed starting alcohol **2**, more NaH (10.8 mg, 270 μ mol, 60% in oil) and bromide **17** (24 mg, 87 μ mol) was added at RT and stirring of the red solution was continued at RT overnight. The solvents were removed *in vacuo* and the residue first purified by flash chromatography (alumina, DCM) and then by prepTLC (silica gel, DCM/MeOH/Et₃N 96:3:1). To remove traces of Et₃N the product was taken up in little H₂O and extracted with DCM. Drying the DCM layer over Na₂SO₄ and evaporation gave **4** (13.9 mg, 27%). UV/Vis (PBS buffer): λ_{max} abs. 264 nm. IR: 2925, 2850, 1657, 1530, 1309, 1278, 1176, 1104, 924, 733, 704 cm⁻¹. ¹H-NMR (300 MHz, CDCl₃) δ 8.38 (d, *J* = 8.1, 1H), 7.84 – 7.76 (m, 4H), 7.64 – 7.55 (m, 1H), 7.53 – 7.34 (m, 7H), 7.27 (m, 1H), 6.85 (d, *J* = 8.1, 1H), 4.66 – 4.47 (m, 5H), 3.44 (t, *J* = 5.7, 2H), 3.17 (d, *J* = 10.5, 2H), 2.63 – 2.45 (m, 5H), 2.33 – 2.22 (m, 2H), 2.07 – 1.93 (m, 3H), 1.63 – 1.43 (m, 3H), 1.14 (d, *J* = 9.0 Hz, 2H). ¹³C-NMR (75 MHz, CDCl₃) δ 196.5, 162.3, 143.1, 141.4, 137.8, 137.1, 132.6, 130.5, 130.2, 128.5, 127.3, 126.9, 123.2, 122.9, 122.7, 109.3, 77.4, 72.7, 67.2, 51.8, 46.1, 40.8, 40.6, 32.6, 30.1, 25.1, 14.2. HRMS *m/z* calcd for C₃₄H₃₉N₄O₃ [M+H]⁺ 551.3017, found 551.3011.

***N*-((1*R*,3*r*,5*S*)-9-Methyl-9-azabicyclo[3.3.1]nonan-3-yl)-1-(3-(4-(3-(trifluoromethyl)-3*H*-diazirin-3-yl)benzamido)propyl)-1*H*-indazole-3-carboxamide (**5**).**³⁹ Amine **3**³⁵ (28.4 mg, 66 μ mol) was dissolved in dry DMF/DCM 3:2 (5 mL) and then carboxylic acid **20** (15.3 mg, 66 μ mol), HATU (50.4 mg, 133 μ mol) and three drops of Et₃N were added. The reaction mixture was stirred at RT overnight. Solvents were removed under reduced pressure and the brown residue was taken up in sat. aq. NaHCO₃ (15 mL) and extracted with DCM (3 x 15 mL). The crude oil obtained after evaporation of the organic layers was purified by prepTLC (silica gel, DCM/MeOH/Et₃N 96:3:1). The product still contained some Et₃N which was removed by dissolving in sat. aq. NaHCO₃ (2 mL) and extracting with DCM (3 x 2 mL). The DCM layers were dried (Na₂SO₄) and evaporated to yield probe **5** (9 mg, 24%) as slightly yellow oil. UV/Vis (PBS buffer): λ_{max} abs. 302 nm. IR: 2924, 1650, 1538, 1345, 1310, 1231, 1154, 940, 842, 743 cm⁻¹. ¹H-NMR (300 MHz, CDCl₃) δ 8.10 (d, *J* = 8.1, 1H), 8.01 (d, *J* = 8.4, 1H), 7.70 (d, *J* = 8.4, 2H), 7.41 – 7.26 (m, 2H), 7.16 – 7.06 (m, 3H), 6.76 – 6.68 (m, 1H), 4.82 (s, 1H), 4.34 (t, *J* = 6.5, 2H), 3.67 (d, *J* =

9.1, 2H), 3.48 – 3.35 (m, 2H), 2.86 (s, 3H), 2.62 (t, $J = 15.3$, 2H), 2.28 – 2.12 (m, 3H), 2.12 – 1.86 (m, 4H), 1.51 (d, $J = 13.5$, 2H), 1.30 – 1.20 (m, 1H), 0.77 (d, $J = 7.5$, 2H). ^{13}C -NMR (75 MHz, CDCl_3) δ 192.2, 166.6, 162.7, 140.8, 137.0, 129.9, 127.5, 127.0, 126.5, 126.1, 122.8, 122.7, 122.2, 109.3, 77.2, 53.5, 46.7, 38.9, 37.6, 30.5, 29.7, 29.0, 24.5, 12.0. HRMS m/z calcd for $\text{C}_{29}\text{H}_{33}\text{F}_3\text{N}_7\text{O}_2$ $[\text{M}+\text{H}]^+$ 568.2642, found 568.2621.

***N*-((1*R*,3*r*,5*S*)-9-Methyl-9-azabicyclo[3.3.1]nonan-3-yl)-1-(3-(4-(4-(prop-2-yn-1-yloxy)benzoyl)benzamido)propyl)-1*H*-indazole-3-carboxamide (6).** Acid **18** (67 mg, 0.24 mmol) was suspended in MeCN (5 mL) and SOCl_2 (128 mg, 1.08 mmol) was added. The mixture was stirred at 80°C for 3 h and then at RT overnight. Volatiles were removed *in vacuo*, the brown residue was redissolved in DCM (5 mL) and cooled to 0°C. A suspension of amine **3**³⁵ (100 mg, 0.218 mmol) in DCM (2 mL) was added at 0°C, the cooling was removed and the reaction mixture stirred at RT overnight. Solvents were evaporated and the crude product purified by flash chromatography (silica gel, DCM/MeOH/ Et_3N 96:3:1). Remaining Et_3N after evaporating the appropriate fractions was removed by dissolving in sat. aq. NaHCO_3 (2 mL) and extracting with DCM (3 x 2 mL). The DCM layers were dried over Na_2SO_4 and evaporated to give probe **6** (15 mg, 11%) as slightly brown oil. UV/Vis (PBS buffer): λ_{max} abs. 296 nm. IR: 2927, 2361, 2161, 1653, 1598, 1539, 1282, 1176, 1024, 930 cm^{-1} . ^1H -NMR (300 MHz, CDCl_3) δ 8.28 (d, $J = 8.2$, 1H), 7.81 – 7.64 (m, 6H), 7.41 – 7.28 (m, 2H), 7.26 – 7.13 (m, 1H), 7.06 – 6.93 (m, 3H), 6.57 (br, 1H), 4.72 (d, $J = 2.4$, 2H), 4.64 – 4.50 (m, 1H), 4.47 (t, $J = 6.5$, 2H), 3.48 (dd, $J = 12.6$, 6.4, 3H), 3.16 (d, $J = 8.9$, 2H), 2.95 (q, $J = 7.3$, 4H), 2.61 – 2.37 (m, 6H), 2.34 – 2.20 (m, 2H), 1.29 (m, 5H). ^{13}C -NMR (75 MHz, CDCl_3) δ 194.6, 166.7, 161.8, 161.4, 140.8, 138.1, 137.2, 132.5, 130.4, 129.8, 127.2, 126.7, 123.2, 123.0, 122.8, 114.7, 108.9, 77.7, 77.2, 76.3, 55.9, 51.5, 47.0, 46.0, 40.8, 40.4, 37.8, 32.8, 29.1, 24.7, 14.2, 9.7. HRMS m/z calcd for $\text{C}_{37}\text{H}_{40}\text{N}_5\text{O}_4$ $[\text{M}+\text{H}]^+$ 618.3075, found 618.3069.

7-(2-Hydroxyethoxy)-1-methyl-*N*-((1*R*,3*r*,5*S*)-9-methyl-9-azabicyclo[3.3.1]nonan-3-yl)-1*H*-indazole-3-carboxamide (8). Hydroxy indazole **7**^{31,35} (133 mg, 0.405 mmol) was dissolved in dry THF/DMF 5:1 (6 mL) and KO^tBu (50 mg, 0.446 mmol) was added. The mixture was cooled to 0°C and

1
2
3 stirred for 30 min. (2-bromoethoxy)(*tert*-butyl)dimethylsilane (114 mg, 0.477 mmol) dissolved in dry
4 THF (1.5 mL) was added, the cooling was removed and the reaction mixture stirred at RT overnight.
5
6 Reaction control by TLC (silica gel, DCM/MeOH/Et₃N 96:3:1) still indicated presence of starting
7 material **7**. More KO^tBu (29 mg, 0.258 mmol) and TBS-protected bromide (46 mg, 0.192 mmol) were
8
9 thus added and stirring at RT continued for 4 h. Solvents were removed under reduced pressure and the
10
11 residue purified by flash chromatography (alumina, gradient DCM 100% to DCM/MeOH 99:1 and then
12
13 DCM/MeOH 95:5) gave the TBS-protected alcohol (153 mg, 78%). ¹H-NMR (300 MHz, CDCl₃) δ 7.91
14
15 (d, *J* = 8.2, 1H), 7.09 (t, *J* = 7.9, 1H), 6.72 (m, 2H), 4.64 – 4.42 (m, 1H), 4.32 (s, 3H), 4.18 (t, *J* = 4.9,
16
17 2H), 4.03 (t, *J* = 4.9, 2H), 3.07 (d, *J* = 10.4, 2H), 2.59 – 2.42 (m, 5H), 2.00 – 1.89 (m, 3H), 1.49 (m, 1H),
18
19 1.35 (t, *J* = 12.4, 2H), 1.04 (d, *J* = 8.4, 2H), 0.84 (s, 9H), 0.08 (s, 6H). ¹³C-NMR (75 MHz, CDCl₃) δ
20
21 162.0, 145.4, 137.3, 133.0, 125.2, 123.2, 115.0, 106.7, 69.9, 61.6, 51.3, 40.7, 39.5, 36.4, 33.1, 31.4, 25.8,
22
23 24.9, 18.3, 14.3, -5.4. HRMS *m/z* calcd for C₂₆H₄₃N₄O₃Si [M+H]⁺ 487.3099, found 487.3091.
24
25
26
27
28

29 To a solution of TBS-protected alcohol from above (153 mg, 0.315 mmol) in THF (5 mL) was
30
31 added a solution of TBAF (165 mg, 0.631 mmol) in THF (1 mL). The reaction mixture was stirred at RT
32
33 for 2 d. H₂O (15 mL) and 2M aq. NaOH (5 mL) were added and the solution extracted with DCM (4 x 20
34
35 mL). The organic layers were dried (Na₂SO₄) and reduced *in vacuo*. Flash chromatography (alumina,
36
37 gradient DCM 100% to DCM/MeOH 19:1) of the residue gave title alcohol **8** (60 mg, 51%). ¹H-NMR
38
39 (300 MHz, CDCl₃) δ 7.80 (d, *J* = 8.2, 1H), 6.96 (t, *J* = 7.9, 1H), 6.68 (d, *J* = 8.4, 1H), 6.56 (d, *J* = 7.5,
40
41 1H), 4.54 – 4.35 (m, 1H), 4.19 (s, 3H), 4.14 – 4.07 (m, 2H), 4.01 – 3.88 (m, 2H), 2.99 (d, *J* = 10.6, 2H),
42
43 2.51 – 2.34 (m, 5H), 1.89 – 1.80 (m, 3H), 1.43 (m, 1H), 1.31 – 1.19 (m, 2H), 0.95 (d, *J* = 9.8, 2H). One
44
45 proton was not detected due to rapid exchange. HRMS *m/z* calcd for C₂₀H₂₉N₄O₃ [M+H]⁺ 373.2234,
46
47 found 373.2242.
48
49
50

51 **7-(3-Hydroxypropoxy)-1-methyl-N-((1*R*,3*r*,5*S*)-9-methyl-9-azabicyclo[3.3.1]nonan-3-yl)-1*H*-**
52
53 **indazole-3-carboxamide (**9**)**. This was synthesized according to the procedure for **8**, using **7**^{31,35} (116 mg,
54
55 0.353 mmol), KO^tBu (44 mg, 0.392 mmol) and (3-bromopropoxy)(*tert*-butyl)dimethylsilane (107 mg,
56
57
58
59
60

0.423 mmol). Aqueous work up with H₂O (10 mL) and DCM (3 x 15 mL) gave the crude product which was purified by flash chromatography (silica gel, DCM/MeOH/Et₃N 96:3:1). Residual Et₃N in the product was removed by extraction (DCM/H₂O) and yielded TBS-protected alcohol (60.7 mg, 34%) as yellowish solid. ¹H-NMR (300 MHz, CDCl₃) δ 7.91 – 7.84 (m, 1H), 7.06 (t, *J* = 7.9, 1H), 6.74 – 6.64 (m, 2H), 4.60 – 4.40 (m, 1H), 4.27 (s, 3H), 4.17 (t, *J* = 6.1, 2H), 3.81 (t, *J* = 6.1, 2H), 3.05 (d, *J* = 10.5, 2H), 2.56 – 2.39 (m, 5H), 2.05 (p, *J* = 6.1, 2H), 1.92 (dd, *J* = 10.6, 3.4, 3H), 1.53 – 1.41 (m, 1H), 1.41 – 1.26 (m, 2H), 1.02 (d, *J* = 9.6, 2H), 0.84 (s, 9H), 0.00 (s, 6H). HRMS *m/z* calcd for C₂₇H₄₅N₄O₃Si [M+H]⁺ 501.3255, found 501.3256.

Following the procedure for **8**, TBS-deprotection was carried out using protected alcohol from above (60 mg, 0.120 mmol) and TBAF (63 mg, 0.240 mmol). Flash chromatography of the crude product (alumina, gradient DCM 100% to DCM/MeOH 19:1) gave title alcohol **9** (39.5 mg, 85%). ¹H-NMR (300 MHz, CDCl₃) δ 7.82 (d, *J* = 7.8, 1H), 7.00 (t, *J* = 7.9, 1H), 6.71 – 6.57 (m, 2H), 4.53 – 4.36 (m, 1H), 4.21 (s, 3H), 4.16 (t, *J* = 6.0, 2H), 3.82 (t, *J* = 6.1, 2H), 2.99 (d, *J* = 10.6, 2H), 2.51 – 2.33 (m, 5H), 2.06 (quin, *J* = 6.1, 2H), 1.95 – 1.77 (m, 3H), 1.42 (d, *J* = 5.5, 1H), 1.34 – 1.20 (m, 2H), 0.96 (d, *J* = 9.9, 2H). One proton was not detected due to rapid exchange.

7-(3-((4-Benzoylbenzyl)oxy)propoxy)-1-methyl-N-((1*R*,3*r*,5*S*)-9-methyl-9-azabicyclo[3.3.1]nonan-3-yl)-1*H*-indazole-3-carboxamide (10**).** Alcohol **9** (19.7 mg, 51.1 μmol) was dissolved in dry THF/DMF 5:1 (3.5 mL), cooled to 0°C and NaH (9 mg, 225 μmol) was added. After stirring for 5 min at 0°C bromide **17** (21 mg, 76 μmol) was added in one portion, the cooling was removed and the reaction mixture stirred at RT overnight. The solvent were removed *in vacuo* and the residue purified by prepTLC (silica gel, DCM/MeOH/Et₃N 96:3:1). Et₃N contaminating the product was removed by aqueous extraction (DCM/H₂O) and finally gave probe **10** (5.9 mg, 20%) as yellowish solid. IR: 2923, 2855, 2361, 1654, 1532, 1507, 1258, 1113, 735, 701, 631 cm⁻¹. ¹H-NMR (300 MHz, CDCl₃) δ 7.92 (d, *J* = 7.7, 1H), 7.80 – 7.70 (m, 4H), 7.63 – 7.55 (m, 1H), 7.52 – 7.40 (m, 4H), 7.10 (t, *J* = 7.9, 1H), 6.79 – 6.70 (m, 2H), 4.62 (s, 2H), 4.60 – 4.44 (m, 1H), 4.30 – 4.19 (m, 5H), 3.75 (t, *J* = 6.1, 2H), 3.11 (d,

$J = 10.5$, 2H), 2.60 – 2.44 (m, 5H), 2.28 – 2.16 (m, 2H), 2.02 – 1.91 (m, 3H), 1.55 – 1.47 (m, 1H), 1.44 – 1.32 (m, 2H), 1.07 (d, $J = 9.9$, 2H). ^{13}C -NMR (75 MHz, CDCl_3) δ 196.3, 162.0, 145.4, 143.0, 137.6, 137.3, 136.9, 132.8, 132.4, 130.3, 130.0, 128.3, 127.1, 125.2, 123.3, 114.9, 106.2, 77.2, 72.5, 67.0, 65.1, 51.4, 40.6, 39.5, 32.9, 29.7, 29.7, 25.0, 14.3. HRMS m/z calcd for $\text{C}_{35}\text{H}_{41}\text{N}_4\text{O}_4$ $[\text{M}+\text{H}]^+$ 581.3122, found 581.3122.

1-Methyl-*N*-((1*R*,3*r*,5*S*)-9-methyl-9-azabicyclo[3.3.1]nonan-3-yl)-7-(2-((4-(3-(trifluoromethyl)-3*H*-diazirin-3-yl)benzyl)oxy)ethoxy)-1*H*-indazole-3-carboxamide (11). This was obtained following the procedure for **10**, using alcohol **8** (30 mg, 80.6 μmol), NaH (10 mg, 250 μmol) and diazirine bromide **19** (40 mg, 100 μmol). The crude product was purified by prepTLC (silica gel, DCM/MeOH/ Et_3N 96:3:1) and residual Et_3N removed from the product by aqueous extraction (DCM/ H_2O). This yielded probe **11** (16.1 mg, 35%). IR: 2924, 2864, 2358, 2161, 2029, 1977, 1653, 1533, 1258, 1153, 938, 668 cm^{-1} . ^1H -NMR (300 MHz, CDCl_3) δ 7.87 (d, $J = 7.8$, 1H), 7.31 (d, $J = 8.5$, 2H), 7.11 (d, $J = 8.1$, 2H), 7.07 – 6.99 (m, 1H), 6.69 (d, $J = 8.4$, 1H), 6.64 (d, $J = 7.5$, 1H), 4.56 (s, 2H), 4.52 – 4.40 (m, 1H), 4.29 – 4.16 (m, 5H), 3.89 – 3.81 (m, 2H), 3.04 (d, $J = 10.1$, 2H), 2.54 – 2.37 (m, 5H), 1.96 – 1.84 (m, 3H), 1.46 (d, $J = 5.8$, 1H), 1.40 – 1.23 (m, 2H), 1.00 (d, $J = 9.2$, 2H). ^{13}C -NMR (75 MHz, CDCl_3) δ 177.1, 162.1, 145.3, 139.9, 137.51, 133.1, 128.8, 128.0, 126.8, 125.4, 123.3, 115.5, 106.8, 77.4, 72.7, 68.9, 67.8, 51.5, 40.8, 39.6, 33.2, 25.1, 14.5. HRMS m/z calcd for $\text{C}_{29}\text{H}_{34}\text{F}_3\text{N}_6\text{O}_3$ $[\text{M}+\text{H}]^+$ 571.2639, found 571.2640.

(1*R*,3*r*,5*S*)-9-(4-(3-(Trifluoromethyl)-3*H*-diazirin-3-yl)benzyl)-9-azabicyclo[3.3.1]nonan-3-amine (13). Granatane **12**⁴⁰ (30 mg, 0.125 mmol) was dissolved in EtOH (4 mL) and K_2CO_3 (35 mg, 0.253 mmol) and diazirine iodide **21** (40 mg, 0.098 mmol) were added. The suspension was first stirred at RT overnight and then heated at 55°C for 3.5 h. The solvent was reduced to about 2 mL *in vacuo*, DCM (10 mL) was added and the mixture extracted with H_2O . The water phases were washed with DCM (2 x 10 mL). The combined organic layers were dried over Na_2SO_4 and evaporated. The crude product was purified by flash chromatography (silica gel, gradient hexanes 100% to hexanes/EtOAc 99:1 to hexanes/EtOAc 7:3) and gave the *N*-alkylated granatane (36 mg, 82%). ^1H -NMR (300 MHz, CDCl_3) δ

7.31 (d, $J = 6.9$, 2H), 7.05 (d, $J = 7.3$, 2H), 4.22 (s, 1H), 4.01 (s, 1H), 3.73 (s, 2H), 2.95 (d, $J = 10.5$, 2H), 2.29 (dd, $J = 17.9$, 12.0, 2H), 1.83 (d, $J = 2.9$, 3H), 1.39 (s, 9H), 1.22 (s, 1H), 1.08 (t, $J = 12.6$, 2H), 0.93 (d, $J = 10.1$, 2H). ^{13}C -NMR (75 MHz, CDCl_3) δ 142.5, 128.6, 127.4, 126.4, 79.1, 77.2, 55.4, 49.4, 33.9, 29.7, 28.5, 24.8, 14.2, 14.1. HRMS m/z calcd for $\text{C}_{22}\text{H}_{30}\text{F}_3\text{N}_4\text{O}_2$ $[\text{M}+\text{H}]^+$ 439.2315, found 439.2316.

To a solution of Boc-protected granatane from above (30 mg, 0.068 mmol) in DCM (1 mL) was added TFA (0.25 mL) and the reaction mixture stirred at RT for 6 h. The volatiles were removed *in vacuo*, the residue taken up in DCM (6 mL) and extracted with sat. aq. NaHCO_3 (3 mL). The aqueous phase was extracted with DCM (3 x 4 mL), the combined organic layers dried over Na_2SO_4 and evaporated. This gave title compound **13** (24.5 mg, quant.). ^1H -NMR (300 MHz, CDCl_3) δ 7.29 (d, $J = 8.5$, 2H), 7.05 (d, $J = 8.0$, 2H), 3.74 (s, 2H), 3.33 – 3.16 (m, 1H), 2.92 (d, $J = 11.4$, 2H), 2.18 (td, $J = 11.2$, 5.7, 2H), 1.93 – 1.72 (m, 3H), 1.48 – 1.38 (m, 1H), 1.12 – 0.99 (m, 2H), 0.94 (d, $J = 12.9$, 2H). Two protons (amine) were not observed due to rapid exchange. ^{13}C -NMR (75 MHz, CDCl_3) δ 142.9, 128.5, 127.4, 126.3, 122.2 (q, $J = 274.7$), 55.4, 49.6, 43.0, 37.3, 29.7, 24.9, 14.2. HRMS m/z calcd for $\text{C}_{17}\text{H}_{22}\text{F}_3\text{N}_4$ $[\text{M}+\text{H}]^+$ 339.1791, found 339.1780.

***N*-((1*R*,3*r*,5*S*)-9-(4-(3-(Trifluoromethyl)-3*H*-diazirin-3-yl)benzyl)-9-azabicyclo[3.3.1]nonan-3-yl)-1*H*-indazole-3-carboxamide (14).** Indazole-3-carboxylic acid (19.4 mg, 0.12 mmol), DCC (27.4 mg, 0.133 mmol) and HOBt (15 mg, 0.111 mmol) were dried in high-vacuum for 20 min and then dissolved under dry conditions in DCM/DMF 3:2 (5 mL). After stirring the solution for 2 h at RT, granatane **13** (22.8 mg, 0.067 mmol) dissolved in DCM (3 mL) was added dropwise and the reaction mixture stirred at RT overnight. The solvents were removed under reduced pressure, the residue dissolved in DCM (5 mL) and extracted with sat. aq. NaHCO_3 (3 mL). The aqueous phase was extracted with DCM (3 x 6 mL), the combined organic layers dried (Na_2SO_4) and evaporated. The crude product was purified by flash chromatography (silica gel, DCM/MeOH/ Et_3N 96:3:1) and prepHPLC (reverse phase, gradient H_2O 100% + 0.1% TFA to H_2O /MeCN 4:6 + 0.1% TFA to MeCN 100% + 0.1% TFA, t_R (product) = 28 min). The fractions were lyophilized, the isolated TFA salt dissolved in H_2O (1 mL) and extracted into CHCl_3 (3

mL). Evaporation of the organic phase gave indazole carboxamide **14** (21.6 mg, 66%). ¹H-NMR (300 MHz, CDCl₃) δ 10.78 (br, 1H), 8.37 (d, *J* = 8.1, 1H), 7.45 (d, *J* = 8.4, 1H), 7.40 – 7.29 (m, 3H), 7.28 – 7.19 (m, 1H), 7.04 (d, *J* = 8.0, 2H), 6.83 (d, *J* = 8.7, 1H), 4.71 – 4.45 (m, 1H), 3.77 (s, 2H), 3.00 (d, *J* = 11.1, 2H), 2.41 (td, *J* = 11.9, 6.2, 2H), 1.94 – 1.80 (m, 3H), 1.49 (d, *J* = 9.4, 1H), 1.35 – 1.21 (m, 2H), 0.97 (d, *J* = 10.9, 2H). ¹³C-NMR (75 MHz, CDCl₃) δ 162.3, 157.1, 142.5, 141.5, 139.5, 128.7, 127.5, 127.2, 126.4, 122.7 (d, *J* = 2.7), 122.2 (q, *J* = 274.3), 122.0, 109.9, 55.5, 53.4, 49.3 (d, *J* = 7.7), 41.3, 33.9, 33.5, 28.1, 25.6, 24.9 (d, *J* = 6.6), 14.2. HRMS *m/z* calcd for C₂₅H₂₆F₃N₆O [M+H]⁺ 483.2115, found 483.2100.

1-methyl-*N*-((1*R*,3*r*,5*S*)-9-(4-(3-(Trifluoromethyl)-3*H*-diazirin-3-yl)benzyl)-9-azabicyclo[3.3.1]nonan-3-yl)-1*H*-indazole-3-carboxamide (15). Indazole carboxamide **14** (16 mg, 0.033 mmol) was dissolved in THF/DMF 4:1 (3 mL), KO^tBu (5 mg, 0.043 mmol) and MeI (15 mg, 1.06 mmol) were added and the reaction mixture stirred at RT overnight. Solvents were removed under reduced pressure and the residue taken up in EtOAc (7 mL). This was extracted with sat. aq. NaCl (3 mL), sat. aq. NaHCO₃ (3 mL) sat. aq. NH₄Cl (3 mL) and finally sat. aq. NaCl (3 mL). The organic layer was dried over Na₂SO₄ and evaporated yielding probe **15** (14.5 mg, 88%). UV/Vis (PBS buffer): λ_{max} abs. 327 nm. ¹H-NMR (300 MHz, CDCl₃) δ 8.39 – 8.27 (m, 1H), 7.41 – 7.32 (m, 4H), 7.25 – 7.20 (m, 1H), 7.07 (d, *J* = 7.9, 2H), 6.73 (d, *J* = 8.7, 1H), 4.70 – 4.49 (m, 1H), 4.02 (s, 3H), 3.80 (s, 2H), 3.03 (d, *J* = 11.2, 2H), 2.43 (td, *J* = 12.1, 6.4, 2H), 2.01 – 1.77 (m, 3H), 1.53 (br, 1H), 1.39 – 1.25 (m, 2H), 1.00 (d, *J* = 13.0, 2H). ¹³C-NMR (100 MHz, CD₃OD) δ 164.1, 141.9, 128.1, 126.8, 126.2, 125.8, 122.4, 122.0, 108.4, 54.8, 48.8, 40.5, 35.3, 32.9, 24.2, 20.5, 15.4. HRMS *m/z* calcd for C₂₆H₂₈F₃N₆O [M+H]⁺ 497.2271, found 497.2262.

1-(Prop-2-yn-1-yl)-*N*-((1*R*,3*r*,5*S*)-9-(4-(3-(trifluoromethyl)-3*H*-diazirin-3-yl)benzyl)-9-azabicyclo[3.3.1]nonan-3-yl)-1*H*-indazole-3-carboxamide (16). Indazole carboxamide **14** (24 mg, 0.05 mmol) was dissolved in DMF (1 mL) under dry conditions, Cs₂CO₃ (42.7 mg, 0.131 mmol) was added and the solution stirred at RT 20 min. 3-Bromoprop-1-yne (8.2 mg, 0.068 mmol) was added and the

reaction mixture stirred at RT for 4 h. Solvents were removed *in vacuo*, sat. aq. NaHCO₃ (5 mL) was added and extracted with DCM (3 x 20 mL). The combined organic layers were dried (Na₂SO₄) and evaporated to give probe **16** (24.2 mg, 93%). UV/Vis (PBS buffer): λ_{max} abs. 316 nm. IR: 3309, 2926, 2359, 2343, 1642, 1539, 1343, 1311, 1231, 1181, 1154, 937 cm⁻¹. ¹H-NMR (300 MHz, DMSO-d₆) δ 8.22 (d, *J* = 8.1, 1H), 8.15 (d, *J* = 9.1, 1H), 7.81 (d, *J* = 8.5, 1H), 7.52 (m, 3H), 7.34 (d, *J* = 7.3, 1H), 7.29 (d, *J* = 8.6, 2H), 5.58 (d, *J* = 7.8, 1H), 5.44 (d, *J* = 2.4, 2H), 4.58 – 4.42 (m, 1H), 3.89 (s, 2H), 3.02 (d, *J* = 10.8, 2H), 2.26 – 2.11 (m, 3H), 1.92 (t, *J* = 14.1, 2H), 1.80 – 1.40 (m, 4H), 1.00 (d, *J* = 15.8, 2H). ¹H-NMR (300 MHz, CDCl₃) δ 8.36 (d, *J* = 8.2, 2H), 7.49 (d, *J* = 8.5, 1H), 7.36 – 7.41 (m, 3H), 7.25 (m, 1H), 7.07 (d, *J* = 8.0, 2H), 6.73 (d, *J* = 8.7, 1H), 5.12 (d, *J* = 2.5, 2H), 4.67 – 4.52 (m, 1H), 4.02 (d, *J* = 7.9, 1H), 3.48 – 3.34 (m, 1H), 3.03 (d, *J* = 10.9, 2H), 2.52 – 2.39 (m, 2H), 2.37 (t, *J* = 2.5, 1H), 1.94 – 1.80 (m, 2H), 1.68 – 1.45 (m, 2H), 1.40 – 1.28 (m, 2H), 1.03 – 0.93 (m, 2H). ¹³C-NMR (75 MHz, CDCl₃) δ 161.7, 156.7, 142.5, 140.6, 138.5, 128.7, 127.4, 126.5, 123.5, 122.9, 120.4, 109.4, 77.2, 76.5, 74.3, 55.5, 49.3, 41.2, 39.4, 34.0, 33.5, 25.6, 24.9, 14.3. ¹⁹F-NMR (376 MHz, DMSO-d₆) δ -64.6. HRMS *m/z* calcd for C₂₈H₂₈F₃N₆O [M+H]⁺ 521.2271, found 521.2267.

Biology. Materials, human embryonic kidney (HEK) 293T cell culture maintenance, 5-HT₃ receptor expression, 5-HT₃ receptor affinity purification and its micelle-solubilization, radioligand binding and binding data analysis were described previously.³²

Photo-crosslinking 5-HT₃ receptor with granisetron probes. For all irradiation experiments a UVP 3UVTM – 38 UV Lamp (Upland, CA, USA) was used and set to an irradiation wavelength of 302 nm (lamp power: 8W).

For whole cell lysate experiments, HEK293T cells stably expressing human N-terminal FLAG-tagged 5-HT_{3A} receptor³² were defrosted (1.8 mL) and 2 mL PBS buffer (50 mM NaCl, 0.27 mM KCl, 1 mM Na₂HPO₄, 0.2 mM KH₂PO₄, pH 7.4), 75 μ L HaltTM Protease Inhibitor Cocktail (1x, Thermo Fisher Scientific), 5 μ L CyanaseTM Nuclease (50 U/ μ L, RiboSolutions Inc.) and 5 μ L MnSO₄ (1 M) was added. The cells were homogenized using a Dounce homogenizer, and by aspiration with a syringe through a

21G needle and expulsion through a 27G needle. 5-HT₃ receptor-containing whole cell lysate (250 μ L) prepared in this way was incubated either with 2.5 μ L **6** (25 mM in DMSO), 2.5 μ L **16** (25 mM in DMSO) or 2.5 μ L **22** (50 mM in DMSO) at RT for 90 min in the dark and then irradiated on ice for 30 min in a 9-well plate. The solutions were transferred back to tubes and 250 μ L PBS was added.

To determine concentration dependence of photo-crosslinking with **6**, a solution of purified, micelle-solubilized FLAG-tagged *h*5-HT₃A receptor was adjusted to a concentration of 8.4 μ g/mL using PBS buffer + 0.4 mM C₁₂E₉. In a 48-well plate, 5-HT₃ receptor-micelle solutions (100 μ L) were mixed each with 1 μ L of different stock solutions of either **6** or **22** in order to obtain final compound concentrations of 2.5 μ M, 250 nM, 25 nM and 2.5 nM. The solutions were incubated in the dark for 30 min at RT and then irradiated on ice for 30 min. The samples were diluted with 50 μ L PBS and transferred back from the wells into tubes.

For competition experiments with granisetron, a solution of purified, micelle-solubilized FLAG-tagged *h*5-HT₃A receptor was adjusted to a concentration of 50 μ g/mL using PBS buffer + 0.4 mM C₁₂E₉. Using a 48-well plate, 100 μ L of this 5-HT₃ receptor-micelle solution was mixed with 0.5 μ L granisetron (2.5 mM in DMSO) and incubated for 10 min at RT. Subsequently, either 0.5 μ L **6** (25 mM in DMSO) or 0.5 μ L **22** (50 mM) was added and the samples incubated for further 30 min in the dark at RT. The samples were then irradiated on ice for 20 min, diluted with PBS (50 μ L) and transferred back to tubes.

For live cells irradiation experiments, HEK293T cells stably expressing human N-terminal FLAG-tagged 5-HT₃A receptor were grown to approximately 80% density in four T300 plates. The cells were washed with PBS (10 mL/plate), then incubated with PBS (10 mL/plate) for 10 min at 37°C and detached by repeatedly flushing them off. The cell suspension was cooled on ice, 300 μ L Halt™ Protease Inhibitor Cocktail added and split into two portions to which probes **6** or **22** were added (100 μ L, 0.5 mM in DMSO). The suspensions were incubated for 15 min at RT in the dark and then irradiated in a 6-well plate on ice for 25 min while gently stirring the cells. The viability of the cells was monitored during irradiation (*t* = 0, 10, 20, 25 min) by using a cell counter (Countess automated cell counter, Invitrogen)

and is depicted in Figure S2. For each cell suspension portion (with either **6** or **22**), the cells were pelleted by centrifugation (5 min, 500g), the supernatant discarded and the volume increased to 3 mL with PBS buffer. More protease inhibitor cocktail was added (75 μ L) and the cells were homogenized first using a 5 mL-douncer, and then by aspiration with a syringe through a 21G needle and expulsion through a 27G needle. The membranes were collected by centrifugation at 100,000g for 30 min, pellets resuspended in 5 mL solubilization buffer (10 mM phosphate buffer, pH 7.4, 0.5 M NaCl, 10 mM imidazole, 2 mM C₁₂E₉) and 2.5 μ L Cyanase (50 U/mL) and 2.5 μ L MnSO₄ (1 mM) were added. The samples were agitated for 1 h at 4°C and then centrifuged (1 h, 100,000g) to remove insoluble components. The supernatant was incubated head-over-tail with 100 μ L prewashed FLAG beads (FLAG M2 agarose beads, Sigma) for 2 h at 4°C. The beads were removed by centrifugation (2 min, 500g), washed 5 times with PBS buffer containing 0.4 mM C₁₂E₉ and incubated with 125 μ L elution buffer (wash buffer supplemented with 1 mg/mL FLAG peptide). The suspension was centrifuged (2 min, 500g) through Micro Bio-Spin columns and gave the eluate.

Conjugation with biotin tag via CuAAC. Stock solutions of click reagents biotin-PEG₂-azide **23** (5 mM in DMSO), TCEP (50 mM in H₂O, freshly prepared prior to each experiment), TBTA (1.7 mM in *t*-BuOH/DMSO 4:1) and CuSO₄·5 H₂O (50 mM in H₂O) were prepared and added in this order to a tube containing alkynylated protein sample obtained from photo-crosslinking with either **6**, **16** or **22**. A ratio of photo-crosslinking probe/biotin azide/TCEP/TBTA/CuSO₄ of 1:1000:1000:3000:1000 was normally used and the tube vortexed after addition of each click reagent. The mixture was incubated for 2 h at RT on a vertical rotator and subsequently transferred to a Slide-A-Lyzer[®] MINI Dialysis device (Thermo Fisher, 0.5 mL, 20K MWCO). The protein reaction mixture was dialyzed against PBS buffer (13.5 mL, twice for 2 h at RT, then overnight at 4°C). For biotin pull-down, PBS buffer pre-washed (2 x 25 μ L) Dynabeads[®] MyOne[™] Streptavidin M 270 (Life Technologies[™]) were transferred with PBS (50 μ L) to the dialyzed eluate and incubated overnight. The beads were collected by means of magnet and the supernatant removed. The streptavidin beads were washed with 1 mL C₁₂E₉ solution (2 mM in PBS), then PBS (3 x 1

mL) and incubated with 80 μ L LDS loading buffer (containing 2 mM biotin) for 10 min at 95°C for SDS gel analysis.

Western blot. The protein samples from irradiation and subsequent biotinylation experiments were loaded and run on a SDS-PAGE gel. Protein bands were transferred to a membrane using iBlot[®] Novex[®] Gel Transfer Stacks. Membranes were blocked for 30 min with SeaBlock blocking buffer at RT and then incubated with IRDye 800CW streptavidin (Li-Cor[®], diluted 1:10000 in Seablock buffer + 0.2% SDS) for 30 min. The membranes were washed with TBS-Tween buffer (5 x 5 min), then blocked with TBS-Tween milk (0.1% Tween-20, 5% skim milk powder) for 30 min and incubated with rabbit α -FLAG (Bethyl Laboratories, diluted 1:2000 in TBS-Tween milk) overnight at 4°C. Membranes were rinsed with TBS-Tween (5 x 5 min) and then incubated with donkey α -rabbit IRDye 680 (Li-Cor[®], diluted 1:10000 in TBS-Tween milk) for 2 h at RT. The membranes were rinsed with TBS-Tween (5 x 5 min), dried and then imaged using a Li-Cor[®] Odyssey[®] Fluorescent Imaging System.

Protein Mass Spectrometry. Protein mixtures from photo-crosslinking experiments were run on a SDS-PAGE gel, the gel was fixed for 10 min with H₂O/MeOH/AcOH 5:4:1, washed with H₂O (3 x 5 min) and then stained with Colloidal Coomassie for 2 h. The gel was rinsed with H₂O for 1 h and protein bands between 50 and 60 kDa cut out under sterile conditions. Gel cubes were washed with 50 mM Tris/HCl pH 8 (Tris buffer) and Tris buffer/MeCN 50:50 before disulphide reduction with 50 mM DTT (Fluka, Buchs, Switzerland) in Tris buffer for 30 min at 37°C and subsequent thiol alkylation with 50 mM iodoacetamide (Fluka) in Tris buffer for 30 min at 37°C in the dark. After washing with Tris buffer and dehydration with MeCN the gel cubes were soaked with trypsin solution composed of 10 ng/ μ L trypsin (Promega) in 20 mM Tris/HCl pH 8 + 0.01% ProteaseMax (Promega) for 30 min on ice. Gel cubes were subsequently covered with 5-10 mL of 20 mM Tris/HCl before digestion for 1 h at 50°C. For digestions with Proteinase K (1 ng/ μ L and 10 ng/ μ L, Promega), AspN (10 ng/ μ L, Roche) and LysC/trypsin mix (10 ng/ μ L, Promega), ProteaseMax was not included in the digestion buffer, and incubations were 30 min on ice + 30 min at 37°C, 6 h at 37°C and 16 h at RT, respectively. The supernatant liquid was combined with

a single gel extract performed with 20 mL 20% (v/v) formic acid (Merck) in polypropylene HPLC vials and 5 μ L was analyzed by LC-MS/MS (PROXEON coupled to a QExactive mass spectrometer, ThermoFisher Scientific).

Peptides were trapped on an μ Precolumn C18 PepMap100 (5 μ m, 100 \AA , 300 μ m x 5 mm, ThermoFisher Scientific, Reinach, Switzerland) and separated by backflush on a C18 column (3 μ m, 100 \AA , 75 μ m x 15 cm, Nikkyo Technos, Tokyo, Japan) by applying a 30 min gradient of 5% to 40% MeCN in H₂O, 0.1% formic acid, at a flow rate of 300 nL/min. Peptides of m/z 360-1400 were detected on the QExactive with resolution set at 70,000 with and automatic gain control (AGC) target of 1E06 and maximum ion injection time of 50 ms. A top ten data dependent method for precursor ion fragmentation was applied with the following settings: resolution 17,500, AGC of 1E05, maximum ion time of 110 ms, mass window 2 m/z , collision energy 27, underfill ratio 1%, charge exclusion of unassigned and 1+ ions, peptide match on, respectively.

Fragment spectra information was extracted into mgf file format using ProteomeDiscoverer v1.3 software (ThermoFisher Scientific). Fragment spectra interpretation was performed with ProteomeDiscoverer v1.3 against human database, using fixed modifications of carbamidomethylation on cysteine, and variable modifications of oxidation on methionine, acetylation on protein N-terminal and photo-crosslinking probes on certain amino acids. Protein identifications were considered with at least two unique peptides identified at a 1% FDR on the level of peptide spectrum matches. Fragment peptide sequences were identified with the Sequest HT (v1.3) search engine implemented in the ProteomeDiscoverer software.

Molecular Modelling. Homologous AChBP chimera bound with granisetron (PDB ID: 2YME) was used as a protein template for the docking. This chimera, termed 5HTBP, has substitutions in the orthosteric binding site that mimic the 5-HT₃ receptor.¹⁴ The ligands **4** and **10** were constructed ab initio in Chem3D Pro v14.0 (PerkinElmer, Waltham, MA), based on the crystal structure of granisetron extracted from the Cambridge Structural Database (CSD ID: KUQDAC), and energy-minimized using the

included MM2 force field. A library of 200 conformers was generated for each ligand using OMEGA v2.5 (OpenEye Scientific Software, Santa Fe, NM). To generate a docking template from the 2YME crystal structure, FRED RECEPTOR v2.2.5 (OpenEye Scientific Software) was utilized, whereby the ligand binding site was defined as a box of $V = 5143 \text{ \AA}^3$ around the bound granisetron. The constructed ligands were docked into this binding site template, in order to predict their binding poses, using FRED v2.1 (OpenEye Scientific Software) that utilizes an exhaustive process to position and score all conformers of a ligand at all possible positions within the defined binding site. For each ligand, ten docking poses were generated and ranked using the inbuilt Chemgauss3 scoring function. The proposed binding poses were visualized with PyMOL v1.7 (Schrödinger LLC, Portland, OR).

Associated Content

Supporting Information

Chemistry general procedures and synthesis of photo-crosslinking moieties. Whole cell lysate photo-crosslinking. MS sequence coverage of 5-HT₃A receptor with different digestion protocols. MS/MS of oxidized loop C peptide fragments photo-crosslinked with **4** and **10**. Docking of granisetron into 5HTBP. Alternative docking poses for **4** and **10**. Copies of NMR spectra of final compounds. This material is available free of charge via the internet at <http://pubs.acs.org>.

Abbreviations

AChBP, acetylcholine binding protein; CuAAC, Cu(I)-catalyzed alkyne-azide cycloaddition; ECD, extracellular domain; EM, electron microscopy; GABA, γ -aminobutyric acid (receptor); IBS, irritable bowel syndrome; ICD, intracellular domain; nACh, nicotinic acetylcholine (receptor); PET, positron emission tomography; P-PALM, post-photoaffinity modification; SAR, structure-activity relationship;

SSRIs, selective serotonin reuptake inhibitors; TBTA, tris((1-benzyl-1*H*-1,2,3-triazol-4-yl)methyl)amine; TCEP, tris(2-carboxyethyl)phosphine; TMD, transmembrane domain;

Author Information

Corresponding Author

*M.L.: phone: +41 31 631 3311; fax +41 31 631 4272; E-mail martin.lochner@ibmm.unibe.ch.

Present Author Addresses

[&]M.D.R: United Kingdom Dementia Research Institute at King's College London, Institute of Psychiatry, Psychology and Neuroscience, King's College London, London SE5 9NU, UK.

[†]S.K.V.V: Center for Drug Design, University of Minnesota, Minneapolis, MN 55455, USA.

Author Contributions

T.J. performed the chemical synthesis, protein purification and photo-crosslinking experiments. Mi.L. analyzed the mass spectrometry data and wrote manuscript. M.D.R. established the protein purification and supported T.J. with the photo-crosslinking experiments. A.J.T. measured binding affinity of probes and wrote manuscript. S.B.L. performed protein mass spectrometry analysis and analyzed mass spectrometry data. M.H. supervised protein mass spectrometry and discussed experimental data. M.L. planned and coordinated the study, designed and supervised chemical synthesis and photo-crosslinking experiments, and wrote the manuscript.

Funding Sources

This study was supported by the Swiss National Science Foundation (SNSF professorship PP00P2_123536 and PP00P2_146321 to M.L.) and the British Heart Foundation (PG/13/39/30293 to A.J.T). M.D.R. was supported by the HOLCIM Stiftung zur Förderung der wissenschaftlichen Fortbildung.

Notes

The authors declare no competing financial interest.

Acknowledgments

We thank the analytical services from the Department of Chemistry and Biochemistry, University of Bern, for measuring NMR and MS spectra of synthetic intermediates and final compounds.

References

- (1) Hannon, J., and Hoyer, D. (2008) Molecular biology of 5-HT receptors. *Behav. Brain Res.* 195, 198-213.
- (2) Nichols, D. E., and Nichols, C. D. (2008) Serotonin receptors. *Chem. Rev.* 108, 1614-1641.
- (3) Thompson, A. J. (2013) Recent developments in 5-HT₃ receptor pharmacology. *Trends Pharmacol. Sci.* 34, 100-109.
- (4) Lummis, S. C. R. (2012) 5-HT₃ receptors. *J. Biol. Chem.* 287, 40239-40245.
- (5) Moore, N. A., Sargent, B. J., Manning, D. D., and Guzzo, P. R. (2013) Partial agonism of 5-HT₃ receptors: a novel approach to the symptomatic treatment of IBS-D. *ACS Chem. Neurosci.* 4, 43-47.
- (6) Walstab, J., Rappold, G., and Niesler, B. (2010) 5-HT₃ receptors: role in disease and target of drugs. *Pharmacol. Ther.* 128, 146-169.
- (7) Machu, T. K. (2011) Therapeutics of 5-HT₃ receptor antagonists: current uses and future directions. *Pharmacol. Ther.* 130, 338-347.
- (8) Bétry, C., Etiévant, A., Oosterhof, C., Ebert, B., Sanchez, C., and Haddjeri, N. (2011) Role of 5-HT₃ receptors in the antidepressant response. *Pharmaceuticals* 4, 603.
- (9) Joshi, P. R., Suryanarayanan, A., Hazai, E., Schulte, M. K., Maksay, G., and Bikadi, Z. (2006) Interactions of granisetron with an agonist-free 5-HT_{3A} receptor model. *Biochemistry* 45, 1099-1105.

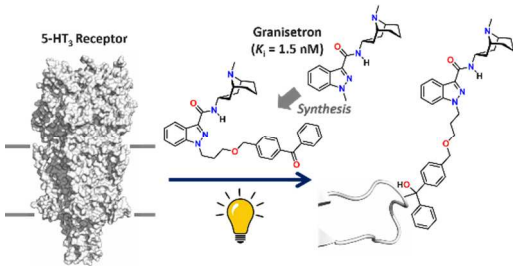
- (10) Nyce, H. L., Stober, S. T., Abrams, C. F., and White, M. M. (2010) Mapping spatial relationships between residues in the ligand-binding domain of the 5-HT₃ receptor using a molecular ruler. *Biophys. J.* 98, 1847-1855.
- (11) Thompson, A. J., Price, K. L., Reeves, D. C., Ling Chan, S., Chau, P.-L., and Lummis, S. C. R. (2005) Locating an antagonist in the 5-HT₃ receptor binding site using modeling and radioligand binding. *J. Biol. Chem.* 280, 20476-20482.
- (12) Hassaine, G., Deluz, C., Grasso, L., Wyss, R., Tol, M. B., Hovius, R., Graff, A., Stahlberg, H., Tomizaki, T., Desmyter, A., Moreau, C., Li, X.-D., Poitevin, F., Vogel, H., and Nury, H. (2014) X-ray structure of the mouse serotonin 5-HT₃ receptor. *Nature* 512, 276-281.
- (13) Basak, S., Gicheru, Y., Samanta, A., Molugu, S. K., Huang, W., Fuente, M. I. d., Hughes, T., Taylor, D. J., Nieman, M. T., Moiseenkova-Bell, V., and Chakrapani, S. (2018) Cryo-EM structure of 5-HT_{3A} receptor in its resting conformation. *Nat. Commun.* 9, 514.
- (14) Kesters, D., Thompson, A. J., Brams, M., van Elk, R., Spurny, R., Geitmann, M., Villalgorido, J. M., Guskov, A., Helena Danielson, U., Lummis, S. C. R., Smit, A. B., and Ulens, C. (2013) Structural basis of ligand recognition in 5-HT₃ receptors. *EMBO Rep.* 14, 49-56.
- (15) Price, K. L., Lillestol, R. K., Ulens, C., and Lummis, S. C. R. (2016) Palonosetron–5-HT₃ receptor interactions as shown by a binding protein cocrystal structure. *ACS Chem. Neurosci.* 7, 1641-1646.
- (16) Ruepp, M.-D., Wei, H., Leuenberger, M., Lochner, M., and Thompson, A. J. (2017) The binding orientations of structurally-related ligands can differ; A cautionary note. *Neuropharmacology* 119, 48-61.
- (17) Hamouda, A. K., Sanghvi, M., Chiara, D. C., Cohen, J. B., and Blanton, M. P. (2007) Identifying the lipid-protein interface of the $\alpha 4\beta 2$ neuronal nicotinic acetylcholine receptor: Hydrophobic photolabeling studies with 3-(trifluoromethyl)-3-(*m*-[¹²⁵I]iodophenyl)diazirine. *Biochemistry* 46, 13837-13846.
- (18) Hamouda, A., Jayakar, S., Chiara, D., and Cohen, J. (2014) Photoaffinity labeling of nicotinic receptors: Diversity of drug binding sites! *J. Mol. Neurosci.* 53, 480-486.
- (19) Nirthanan, S., Ziebell, M. R., Chiara, D. C., Hong, F., and Cohen, J. B. (2005) Photolabeling the *Torpedo* nicotinic acetylcholine receptor with 4-azido-2,3,5,6-tetrafluorobenzoylcholine, a partial agonist. *Biochemistry* 44, 13447-13456.
- (20) Husain, S. S., Stewart, D., Desai, R., Hamouda, A. K., Li, S. G.-D., Kelly, E., Dostalova, Z., Zhou, X., Cotten, J. F., Raines, D. E., Olsen, R. W., Cohen, J. B., Forman, S. A., and Miller, K. W. (2010) *p*-Trifluoromethyldiaziriny-etomidate: A potent photoreactive general anesthetic derivative of etomidate that is selective for ligand-gated ion channels. *J. Med. Chem.* 53, 6432-6444.
- (21) Matsuda, K., Ihara, M., Nishimura, K., Sattelle, D. B., and Komai, K. (2001) Insecticidal and neural activities of candidate photoaffinity probes for neonicotinoid binding sites. *Biosci. Biotechnol. Biochem.* 65, 1534-1541.
- (22) Mortensen, M., Iqbal, F., Pandurangan, A. P., Hannan, S., Huckvale, R., Topf, M., Baker, J. R., and Smart, T. G. (2014) Photo-antagonism of the GABA_A receptor. *Nat. Commun.* 5, 4454.
- (23) Tomizawa, M., Maltby, D., Medzihradsky, K. F., Zhang, N., Durkin, K. A., Presley, J., Talley, T. T., Taylor, P., Burlingame, A. L., and Casida, J. E. (2007) Defining nicotinic agonist binding surface through photoaffinity labelling. *Biochemistry* 46, 8798-8806.
- (24) Yip, G. M. S., Chen, Z.-W., Edge, C. J., Smith, E. H., Dickinson, R., Hohenester, E., Townsend, R. R., Fuchs, K., Sieghart, W., Evers, A. S., and Franks, N. P. (2013) A propofol binding site on mammalian GABA_A receptors identified by photolabeling. *Nat. Chem. Biol.* 9, 715-720.
- (25) Tanaka, Y., Bond, M. R., and Kohler, J. J. (2008) Photocrosslinkers illuminate interactions in living cells. *Mol. Biosyst.* 4, 473-480.
- (26) Dubinsky, L., Krom, B. P., and Meijler, M. M. (2012) Diazirine based photoaffinity labeling. *Bioorg. Med. Chem.* 20, 554-570.

- (27) Nakata, E., Nagase, T., Shinkai, S., and Hamachi, I. (2004) Coupling a natural receptor protein with an artificial receptor to afford a semisynthetic fluorescent biosensor. *J. Am. Chem. Soc.* 126, 490-495.
- (28) Kiyonaka, S., Kato, K., Nishida, M., Mio, K., Numaga, T., Sawaguchi, Y., Yoshida, T., Wakamori, M., Mori, E., Numata, T., Ishii, M., Takemoto, H., Ojiida, A., Watanabe, K., Uemura, A., Kurose, H., Morii, T., Kobayashi, T., Sato, Y., Sato, C., Hamachi, I., and Mori, Y. (2009) Selective and direct inhibition of TRPC3 channels underlies biological activities of a pyrazole compound. *Proc. Natl. Acad. Sci. U. S. A.* 106, 5400-5405.
- (29) Sanghvi, M., Hamouda, A. K., Davis, M. I., Morton, R. A., Srivastava, S., Pandhare, A., Duddempudi, P. K., Machu, T. K., Lovinger, D. M., Cohen, J. B., and Blanton, M. P. (2009) Hydrophobic photolabeling studies identify the lipid-protein interface of the 5-HT₃A receptor. *Biochemistry* 48, 9278-9286.
- (30) Lummis, S. C. R., and Baker, J. (1997) Radioligand binding and photoaffinity labelling studies show a direct interaction of phenothiazines at 5-HT₃ receptors. *Neuropharmacology* 36, 665-670.
- (31) Simonin, J., Vernekar, S. K. V., Thompson, A. J., Hothersall, J. D., Connolly, C. N., Lummis, S. C. R., and Lochner, M. (2012) High-affinity fluorescent ligands for the 5-HT₃ receptor. *Bioorg. Med. Chem. Lett.* 22, 1151-1155.
- (32) Jack, T., Simonin, J., Ruepp, M. D., Thompson, A. J., Gertsch, J., and Lochner, M. (2015) Characterizing new fluorescent tools for studying 5-HT₃ receptor pharmacology. *Neuropharmacology* 90, 63-73.
- (33) Lochner, M., and Thompson, A. J. (2015) A review of fluorescent ligands for studying 5-HT₃ receptors. *Neuropharmacology* 98, 31-40.
- (34) Mu, L., Müller Herde, A., Rüefli, P. M., Sladojevich, F., Milicevic Sephton, S., Krämer, S. D., Thompson, A. J., Schibli, R., Ametamey, S. M., and Lochner, M. (2016) Synthesis and pharmacological evaluation of [¹¹C]granisetron and [¹⁸F]fluoropalonosetron as PET probes for 5-HT₃ receptor imaging. *ACS Chem. Neurosci.* 7, 1552-1564.
- (35) Vernekar, S. K. V., Hallaq, H. Y., Clarkson, G., Thompson, A. J., Silvestri, L., Lummis, S. C. R., and Lochner, M. (2010) Toward biophysical probes for the 5-HT₃ receptor: structure-activity relationship study of granisetron derivatives. *J. Med. Chem.* 53, 2324-2328.
- (36) Patricelli, M. P., and Cravatt, B. F. (2001) Characterization and manipulation of the acyl chain selectivity of fatty acid amide hydrolase. *Biochemistry* 40, 6107-6115.
- (37) Strømgaard, K., Saito, D. R., Shindou, H., Ishii, S., Shimizu, T., and Nakanishi, K. (2002) Ginkgolide derivatives for photolabeling studies: preparation and pharmacological evaluation. *J. Med. Chem.* 45, 4038-4046.
- (38) Hatanaka, Y., Nakayama, H., and Kanaoka, Y. (1993) An improved synthesis of 4-[3-(trifluoromethyl)-3H-diazirin-3-yl]benzoic acid for photoaffinity labeling. *Heterocycles* 35, 997-1004.
- (39) Jack, T., Ruepp, M.-D., Thompson, A. J., Mühlemann, O., and Lochner, M. (2014) Synthesis and characterization of photoaffinity probes that target the 5-HT₃ receptor. *Chimia* 68, 239-242.
- (40) Yang, Z., and Manning, D. D. (2008) 2-Alkylbenzoxazole carboxamides as 5-HT₃ modulators. US2008/0214601 A1.
- (41) Shih, L. B., and Bayley, H. (1985) A carbene-yielding amino acid for incorporation into peptide photoaffinity reagents. *Anal. Biochem.* 144, 132-141.
- (42) Smith, D. P., Anderson, J., Plante, J., Ashcroft, A. E., Radford, S. E., Wilson, A. J., and Parker, M. J. (2008) Trifluoromethyldiazirine: an effective photo-induced cross-linking probe for exploring amyloid formation. *Chem. Commun.*, 5728-5730.
- (43) Bandyopadhyay, S., and Bong, D. (2011) Synthesis of trifunctional phosphatidylserine probes for identification of lipid-binding proteins. *Eur. J. Org. Chem.* 2011, 751-758.
- (44) van Scherpenzeel, M., Moret, E. E., Ballell, L., Liskamp, R. M. J., Nilsson, U. J., Leffler, H., and Pieters, R. J. (2009) Synthesis and evaluation of new thiodigalactoside-based chemical probes to label Galectin-3. *ChemBioChem* 10, 1724-1733.

- (45) Hope, A. G., Peters, J. A., Brown, A. M., Lambert, J. J., and Blackburn, T. P. (1996) Characterization of a human 5-hydroxytryptamine₃ receptor type A (h5-HT_{3R}-A_S) subunit stably expressed in HEK 293 cells. *Br. J. Pharmacol.* 118, 1237-1245.
- (46) Beene, D. L., Brandt, G. S., Zhong, W., Zacharias, N. M., Lester, H. A., and Dougherty, D. A. (2002) Cation- π interactions in ligand recognition by serotonergic (5-HT_{3A}) and nicotinic acetylcholine receptors: The anomalous binding properties of nicotine. *Biochemistry* 41, 10262-10269.
- (47) Duffy, N. H., Lester, H. A., and Dougherty, D. A. (2012) Ondansetron and granisetron binding orientation in the 5-HT₃ receptor determined by unnatural amino acid mutagenesis. *ACS Chem. Biol.* 7, 1738-1745.
- (48) Thompson, A. J., Lester, H. A., and Lummis, S. C. R. (2010) The structural basis of function in Cys-loop receptors. *Q. Rev. Biophys.* 43, 449-499.

Table of Contents Graphic

For Table of Contents Use Only



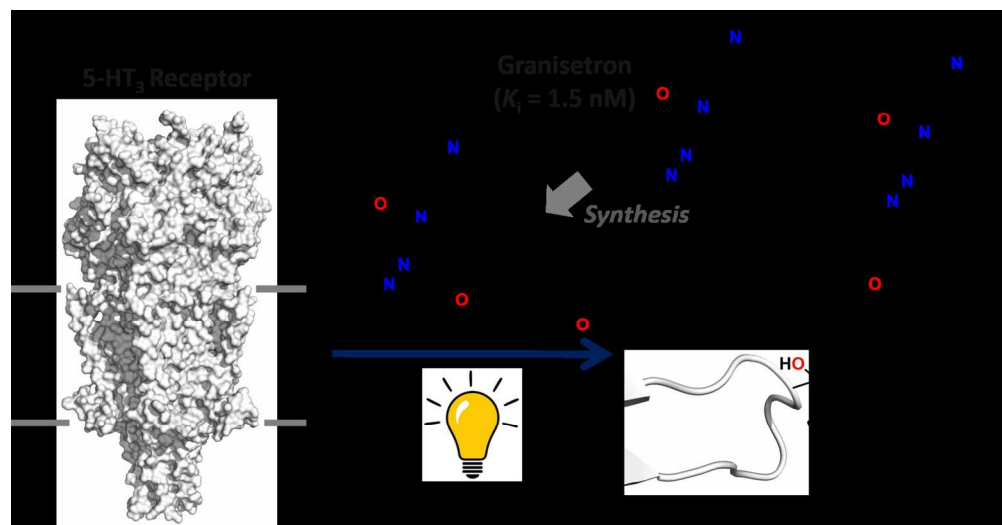


Table of Contents Graphic

308x160mm (150 x 150 DPI)